

# **Aeolian architecture, bedform climbing and preservation space in the Cretaceous Etjo Formation, NW Namibia**

NIGEL MOUNTNEY\* and JOHN HOWELL†

*\*School of Earth Sciences and Geography, Keele University, Keele, Staffordshire ST5 5BG, UK (E-mail: N.P.Mountney@keele.ac.uk)*

*†Stratigraphy Group, Department of Earth Sciences, University of Liverpool, Brownlow Street, Liverpool L69 3BX, UK*

## **ABSTRACT**

Sets of aeolian cross-strata within the Cretaceous Etjo Formation of NW Namibia are bounded by a hierarchy of surfaces, the origin of which are ascribed to one of four processes related to aeolian bedform and erg behaviour. The base of the main aeolian succession is characterized by a basin-wide erosional supersurface that formed in response to a period of aeolian deflation before the onset of the main phase of erg building. Interdune migration surfaces formed by draa migration are planar in sections parallel to the palaeowind and are inclined at up to 5° in an upwind direction (SW). Perpendicular to the palaeowind, interdune surfaces form 500-m-wide troughs, signifying crestline sinuosity within the original bedforms. Superimposition surfaces are inclined at 5–10° in a downwind direction and indicate the migration of crescentic oblique dunes over larger, slipfaceless transverse draa. Reactivation surfaces associated with minor changes in dune slipface orientation are distinct from other bounding surface types because overlying cross-strata lie parallel to them, rather than downlap onto them. Analysis of the geometry of these bounding surfaces, together with the orientation of the cross-strata within the sets that they bound, has enabled the detailed morphology of the original bedforms to be reconstructed. The maximum preserved thickness of individual aeolian sets varies systematically across the basin, from 52 m in the basin depocentre to only 8 m at the basin margin. The set architecture indicates that this spatial variation is primarily the result of decreased angles of bedform climb at the basin margin, rather than the presence of smaller bedforms. Similarly, a temporal reduction in the angle-of-climb, rather than a reduction in bedform size, is considered to be responsible for an upward decrease in preserved set thickness. Reductions in bedform climb angle reflect progressive loss of accommodation space as the accumulating erg filled the basin.

**Keywords** Aeolian, angle-of-climb, bedform, Etjo, Namibia, preservation space.

## **INTRODUCTION**

The purpose of this paper is to examine the three-dimensional stratigraphic architecture of a series of aeolian sandstone bodies in order to understand the sedimentary mechanisms responsible for their deposition and subsequent preservation. Three distinct scales of study have been used to

achieve this goal. First, aeolian architecture has been examined at the laminae scale in order to assess the processes acting on the lee slope of aeolian bedforms at the time of deposition. Secondly, individual outcrop belts have been surveyed at the set scale and portrayed in a series of scaled drawings that depict the geometry and inter-relationship between the various sandstone

bodies and the bounding surfaces that separate them. Thirdly, the semi-regional lateral tracing of prominent bounding surfaces has enabled the aeolian architecture to be placed within the context of the basin-wide evolving erg (sand sea) system. Architectural reconstruction using this multiscale approach has allowed the processes responsible for aeolian lamination and foreset development to be explained with reference to larger scale bedform behaviour, which in turn can be considered with respect to climatic and tectonic controls on basin-wide erg development and preservation.

## STUDY AREA AND GEOLOGICAL SETTING

The Cretaceous Etjo Formation is a 200-m-thick aeolian-dominated succession exposed over an

area of  $\approx 75$  by 40 km in the Huab Basin of north-western Namibia (Frets, 1969; Hodgson, 1970, 1972; Horsthemke *et al.*, 1990; Fig. 1). The Huab Basin forms an eastern extension to the much larger Paraná Basin of South America, which developed throughout the Late Palaeozoic and Mesozoic as an intracratonic basin (Zalan *et al.*, 1991). Subsequently, the basin underwent active extension in Late Jurassic to Early Cretaceous times, before the break-up of West Gondwanaland and the opening of the South Atlantic in the Namibia region (Dingle, 1992; Light *et al.*, 1993; Mountney *et al.*, 1999a). The detailed sedimentology of the Etjo Formation has been described previously by Hodgson (1972), Horsthemke *et al.* (1990) and Mountney *et al.* (1998), who identified four distinct lithological units. From bottom to top these are the Krone Member (coarse clastic material of fluvial origin), the Mixed Aeolian-Fluvial Unit (sandsheet, small aeolian dune and

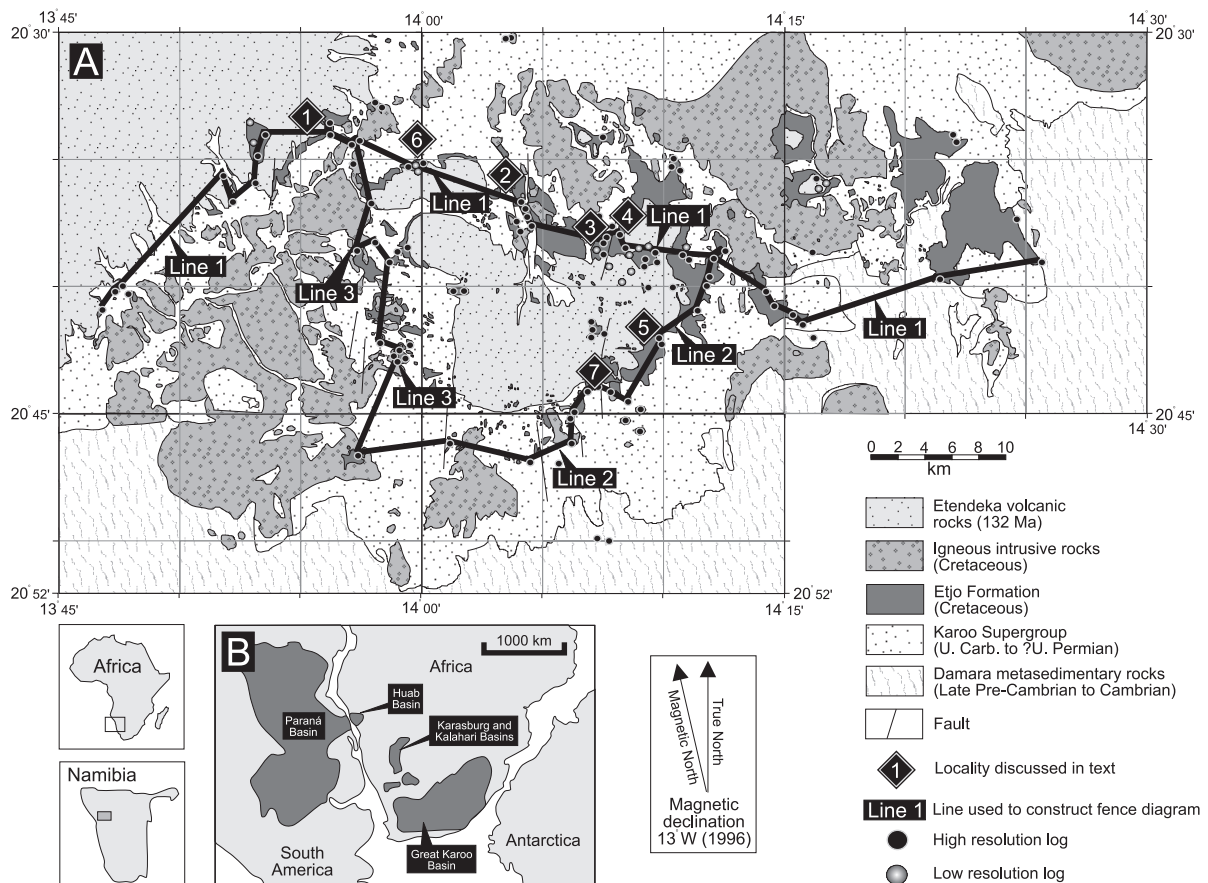


**Fig. 1.** Geological setting of the Huab Basin (NW Namibia). (A) Simplified geological map. High-resolution logs act as control points for the fence diagram presented in Fig. 2, the position of which is shown on the map by solid black lines. Numbered black diamonds show the positions of the main localities discussed in the text. Mapping based on the 1:50 000 geological maps of Horsthemke (1992) and Ledendecker (1992), supplemented with additional interpretation by the authors. (B) Cartoon reconstruction of the West Gondwana region illustrating Late Jurassic palaeogeographic location of the Huab Basin in relation to the Paraná Basin. Modified from Mountney *et al.* (1999a).

ephemeral stream 'fore-erg' deposits; Porter, 1986), the Main Aeolian Unit (aeolian dune and draa deposits) and the Upper Aeolian Unit (aeolian sandstones intercalated with flood basalts). The present study focuses on the Main and Upper Aeolian Units, which are represented by up to 150 m of medium-grained, yellow–white, quartz sandstone, characterized by well-sorted and well-rounded grains that commonly exhibit a 'millet seed' texture. Exposures of these deposits reveal sets of aeolian strata that are delimited by a complex hierarchy of bounding surfaces. The aeolian succession is overlain by in excess of 500 m of Etendeka flood basalts (Milner *et al.*, 1995) that 'drowned' the aeolian erg and, in so doing, preserved complete aeolian bedforms with heights and wavelengths of up to 100 m and 1.3 km respectively (Jerram *et al.*, 1999). The intact preservation of ancient aeolian bedforms at the top of the Etjo Formation enables the original bedform morphology to be related directly to complex bounding surface architectures, thus aiding palaeogeographic reconstructions (Mountney *et al.*, 1999b). The basal Etendeka flood basalts have been radiometrically dated and assigned an age of  $132 \pm 1$  Ma (Renne *et al.*, 1996). These lavas interfinger with the uppermost 100 m of the Etjo Formation, and the aeolian sandstones are therefore also considered to be of Early Cretaceous age.

## DATA SET AND METHODS

The primary data for this study were acquired over a 2-year period using a variety of techniques. The Etjo Formation within the Huab Basin was mapped over an area of 3000 km<sup>2</sup> (Fig. 1). This was achieved using the geological maps of Horsthemke (1992) and Ledendecker (1992) as a template, together with 1:30 000 scale aerial photographs and satellite images. Seventy high-resolution sedimentary logs, with a cumulative length of over 4000 m, record the detailed sedimentology of the Etjo Formation around the basin. In addition, 14 low-resolution logs, with a cumulative total length of 4500 m, record the interaction of the Etjo Formation with the overlying Etendeka flood basalts (Jerram *et al.*, 1999). Both high- and low-resolution logs have been used to construct a series of regional correlation panels that total 148 km in length. The integrity of the interlog correlations summarized on these panels has been tested by 'walking-out' key stratigraphic surfaces between

individual logged section sites. These correlation panels provide a series of two-dimensional slices through the Huab Basin and are here presented as a fence diagram in order to afford a three-dimensional view of the basin architecture (Fig. 2).

At a more detailed scale, a series of nine architectural element analysis (AEA) panels with a cumulative total length of 12 km have been constructed (see Figs 1 and 2 for geographical location). Individual panels vary in lateral extent from 600 to 2500 m and record the detailed sedimentology and stratigraphic architecture of the Etjo Formation. The accurate geometry of the outcrop together with individual set dimensions were measured using a levelling instrument and tape measure. For the scale of the outcrop, lateral measurement error does not exceed 1 m, and vertical measurement error does not exceed 50 cm. Included on these AEA panels are bounding surfaces, sets of cross-strata and other set features including the style of aeolian stratification. In total, 1767 cross-strata and 612 bounding surface inclinations and orientations were measured from various outcrop sites within the study area. These data enable reconstruction of the aeolian system.

## AEOLIAN STRATIFICATION TYPES

The sandstone is arranged into sets and cosets of cross-strata (5–52 m thick), the internal architecture of which is characterized by three basic lamination types: grainflow, grainfall and wind-ripple laminae (Hunter, 1977, 1981).

Grainflow-deposited laminae (Fig. 3A and B) are composed of medium-grained, moderate to well-sorted, steeply dipping (20–30°) cross-laminated units that are typically 3–5 cm in thickness and display inverse grading, although the lack of variance in grain size may preclude this. Individual flows are frequently wedge shaped and may display a down-dip thickening. Where the flows extend down-dip, a concave geometry is commonly developed. Along strike, grainflow deposits form lens-shaped bodies, typically 2–10 m in lateral extent, that pinch at either end and thicken in the middle. Individual flows commonly display a slightly erosive base, particularly when located in the upper third of a set. Although individual grainflows are usually bounded on both their upper and lower surfaces by grainfall laminae, it is not uncommon for them to be stacked together in a compound manner. Grainflow strata account

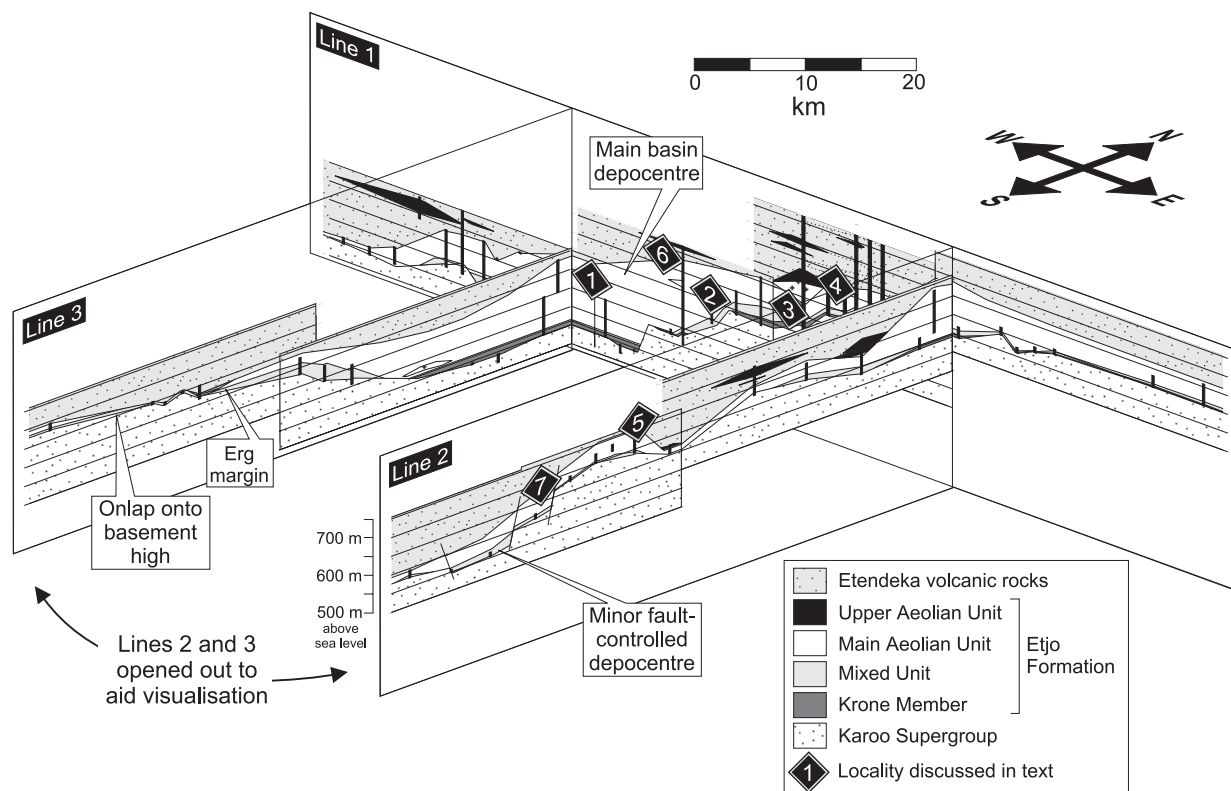


**Fig. 2.** Fence diagram depicting the three-dimensional geometry of the Huab Basin and the gross-scale architecture of the basin fill. Note the progressive thinning of the Main Aeolian Unit of the Etjo Formation from the basin depocentre towards the southern basin margin. Diagram constructed from 50 high-resolution logs and nine low-resolution logs (vertical black columns). Numbered black diamonds show the positions of the main localities discussed in the text. See Fig. 1 for section locations. Vertical exaggeration 50:1. Modified from Moutney *et al.* (1999a).

for 80% of the deposits of the Main and Upper Aeolian Units.

Grainfall-deposited laminae are composed of fine-grained, well-sorted, homogeneous, steeply dipping cross-laminae, which are typically 5 mm in thickness. Individual laminae are tabular and, where bed-scale permits, may be traced both down depositional dip and along strike for tens of metres. Where grainfall laminae are underlain by irregularly bedded horizons, they drape the irregularity rather than lap against its margins (for similar examples, see Anderson, 1988). Grainfall strata account for 10% of the deposits of the Main and Upper Aeolian Units.

Ripple cross-laminated sandstones are characterized by parallel to low-amplitude undulose laminae (up to 5 mm thick). Deposits are commonly bimodally sorted and may display a distinctive pinstripe lamination (Fig. 3C), in which very fine sand and silt is concentrated in the sheltered trough of an advancing ripple (Allen, 1968; Fryberger & Schenk, 1988). Ripple-laminated cross-strata account for 10% of the deposits of the Main and Upper Aeolian Units,

although they are restricted in extent to the basal 0.5–2 m of sets.

## AEOLIAN BOUNDING SURFACES

Bounding surfaces that separate distinct sets of aeolian cross-strata are prominent throughout the Main and Upper Aeolian Units of the Etjo Formation. Establishing the three-dimensional spatial architecture of these bounding surfaces and the stacking of the aeolian sets that they bound is crucial to the accurate reconstruction of the morphology of the original aeolian bedforms. Aeolian bounding surfaces are here assigned to one of three origins related to autocyclic bedform behaviour (Brookfield, 1977; Kocurek, 1996). Bounding surfaces that form in response to the migration of primary bedforms within an erg system are termed interdune migration surfaces (first-order surfaces in the terminology of Brookfield, 1977). Bounding surfaces that form in response to the migration of secondary bedforms over a larger scale primary bedform are termed

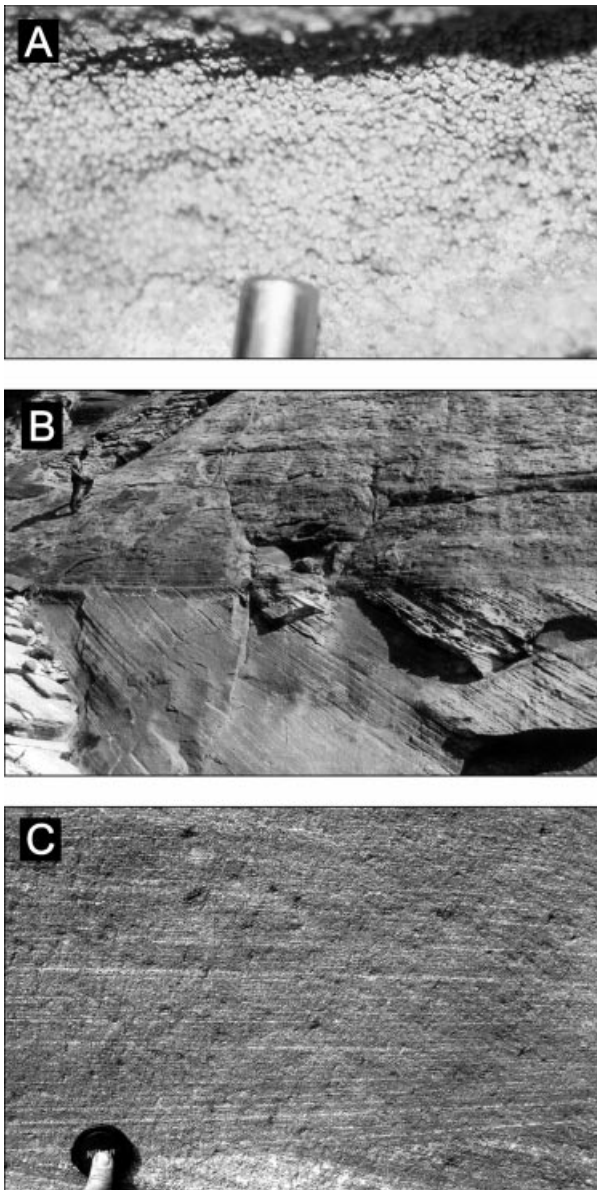


**Fig. 3.** (A) Very well-sorted, well-rounded, highly spherical, medium sandstone of the Main Aeolian Unit exhibiting a ‘millet seed’ texture (pen lid diameter = 5 mm). (B) Cross-stratified grainflow laminae overlain by horizontally laminated wind-ripple strata. Grainflow laminae are 3–5 cm thick, composed of medium sandstone and show slight inverse grading. Person = 1.8 m tall. (C) Bimodally sorted, wind-ripple laminated sandstone displaying ‘pinstripe’ lamination. Lens cap diameter = 5 cm.

superimposition surfaces (second-order surfaces in the terminology of Brookfield, 1977). Bounding surfaces that form in response to changes in bedform slipface orientation (caused, for example, by a change in prevailing wind direction) are termed reactivation surfaces (third-order surfaces

in the terminology of Brookfield, 1977). Kocurek (1996) discussed the criteria for recognizing and differentiating between each of these bounding surface types.

A fourth type of aeolian bounding surface, the supersurface (Talbot, 1985; Kocurek, 1988), may form as a result of the complete or partial termination of ergs or dune-fields. This allocyclic type of bounding surface can result from a variety of factors or events, most notably changes in sand supply, water table or erg activity, each of which may in turn be driven by the underlying mechanisms of climate change, tectonic subsidence/uplift and sea-level change (Kocurek & Havholm, 1993). The correct identification of bounding surface type is crucial for accurate palaeo-environmental reconstruction. In the Etjo Formation, all four principal types of bounding surface are encountered, and their three-dimensional geometric relationships have been used to reconstruct the behaviour and morphology of the original erg system. Sedimentary architectures are described below with reference to the position of the accumulation within the evolving basin.

### STRATIGRAPHY OF THE MAIN AEOLIAN UNIT

The Main Aeolian Unit within the Etjo Formation is defined as a predominantly aeolian succession of strata that overlies red-coloured mixed aeolian and fluvial deposits beneath and is overlain by a mixed aeolian and volcanic accumulation termed the Upper Aeolian Unit (Mountney *et al.*, 1998). The base of the Main Aeolian Unit is defined by a basin-wide surface that is easily recognized in outcrop. Deposits of the Main Aeolian Unit in the Huab Basin vary in thickness from zero at the basin margins to 150 m in the basin depocentre. The set and bounding surface architecture of this unit is described and interpreted with reference to AEA panels from five type localities that occupy various positions within the basin (depocentre, mid-basin region, Huab Outliers and southerly basin margin; Figs 1 and 2).

#### Sedimentary architecture in the basin depocentre (locality 1)

*Description.* The basin depocentre is situated along the course of the present-day Huab River where the Etjo Formation attains a vertical thickness of 200 m. At locality 1, the accumulation is

exposed continuously over a distance of 2.2 km, both parallel (locality 1a) and perpendicular (localities 1b and 1c) to the palaeowind direction (Fig. 4).

The base of the Main Aeolian Unit at locality 1a is marked by an extensive bounding surface exposed continuously over a lateral distance of 1100 m. This surface is characterized by a quartz granule and pebble lag, polygonal fractures that extend downwards from the surface for up to 20 cm into the underlying mixed aeolian and fluvial deposits and a palaeotopography with relief of up to 20 m and local dips of up to 6°. Aeolian sandstones arranged into cross-stratified sets overlie the basal surface. The lowermost set at locality 1a varies in thickness from 45 m to 52 m along the length of the outcrop. The lowermost boundary to this set is defined by the basal bounding surface, whereas the uppermost boundary is characterized by a laterally extensive bounding surface that extends over the length of the outcrop and dips at up to 5° in an upwind direction to the SW. The internal architecture of the basal set in the central part of locality 1a is composed of simple cross-strata that are inclined at 20–24° towards 045° and extend throughout the thickness of the set. Within the basal 2 m of the set, these inclined cross-stratified units merge with a low-angle laminated unit that lies directly on the basal bounding surface. Towards both ends of the outcrop, the internal set architecture is more complex, being characterized by a series of inclined bounding surfaces that dip at 4–10° towards 045°. These surfaces extend continuously from the upper to the lower coset boundary and display a gently concave-up geometry with an asymptotic base where they downlap onto the basal bounding surface. Cross-strata downlap onto, rather than cross-cut, these inclined surfaces (Fig. 4) and exhibit a mean orientation towards 060°.

Overlying sets of cross-strata at locality 1a are thinner than the basal set (10–15 m). At their base, they are characterized by near-horizontal, planar, laterally extensive bounding surfaces that are usually overlain by 1 m of horizontally laminated sandstone. These horizontally laminated deposits pass upwards into cross-strata inclined at 20–24° towards the north to east. The internal architecture of each of these sets is usually simple, being exclusively cross-stratified, but there are examples of compound architectures, in which inclined bounding surfaces subdivide a coset. Where present, these surfaces are inclined at up to 8°, dip down towards the north-east, downlap onto the bounding surface that

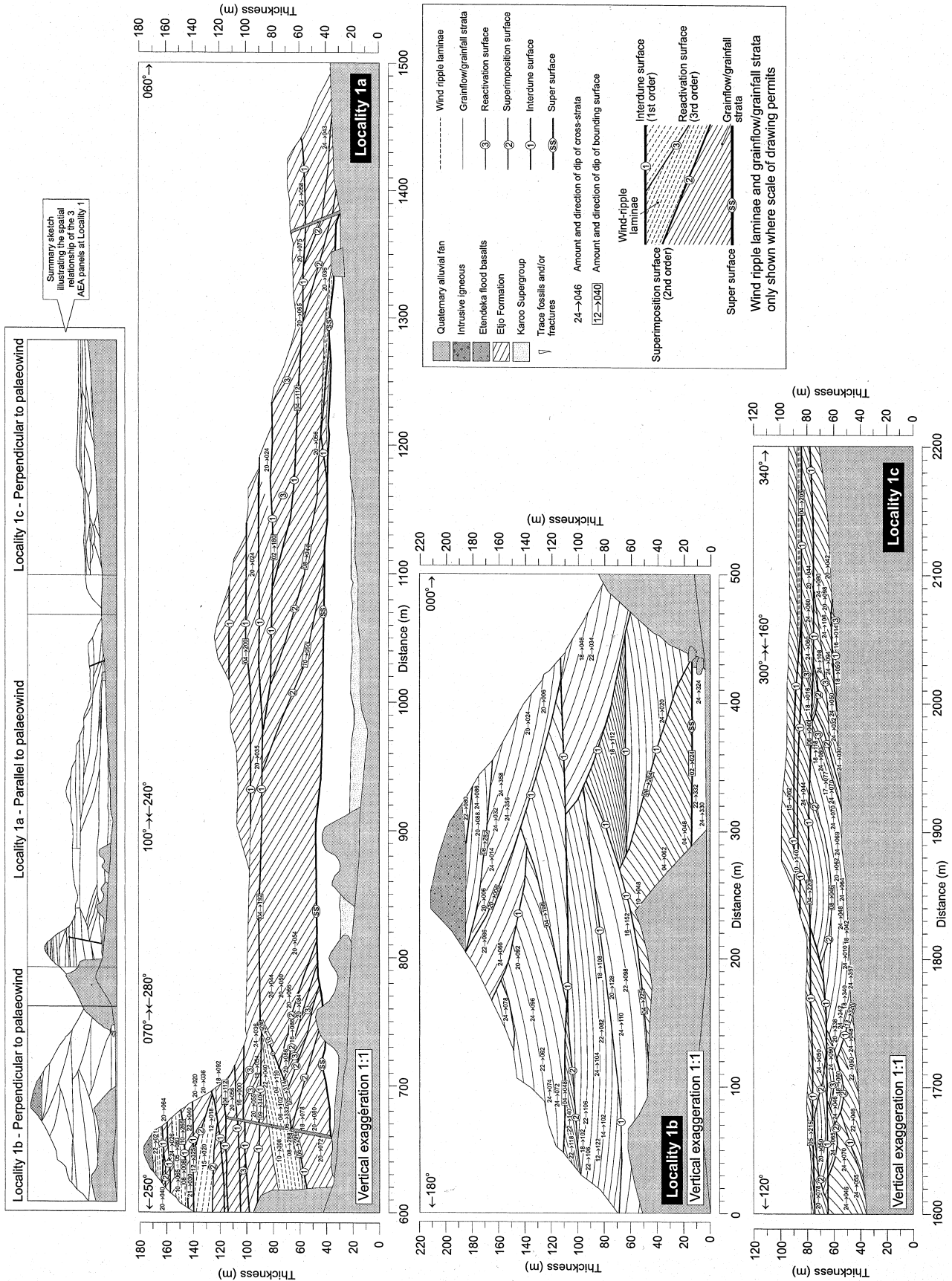
**Fig. 4.** Architectural element analysis panel depicting set geometry and bounding surface relationships at locality 1 (basin depocentre). Locality 1a is oriented parallel to the palaeowind. Note the 50-m-thick coset with internal superimposition surfaces at the base of the succession. Localities 1b and 1c are oriented perpendicular to the palaeowind. Note the troughs of various scales.

defines the base of the coset, are gently concave-up in form and are directly overlain by more steeply inclined cross-stratification planes that downlap onto them.

Localities 1b and 1c (located either side of locality 1a) are cliffs orientated perpendicular to the palaeowind direction that expose a complex stratigraphic architecture. At locality 1b, the basal set is defined at its base by the basal bounding surface and at its top by a series of trough-shaped features that have scoured into and partially eroded the uppermost part of the set (Fig. 4). The maximum preserved thickness of the basal set is 45 m (tapering in each direction), while its internal architecture is dominated by cross-strata inclined at 24° and orientated between north and east. Overlying sets up to 20 m thick are all defined by trough-shaped bounding surfaces that are inclined up to 15°, although dips of 5–8° are more typical. Two large troughs are exposed in their entirety and are 380 m and 500 m wide at their maximum extents (Fig. 4). The remaining troughs are only partially exposed, with only one half typically seen. These 'half-troughs' are typically 200–250 m wide, suggesting a complete trough width of up to 500 m.

Locality 1c also exposes sets bounded by large-scale troughs up to 290 m wide, at least 30 m thick and defined at their base by bounding surfaces inclined at up to 13°. One of these bounding surfaces can be directly correlated with the bounding surface that defines the top of the 52-m-thick set at locality 1a, 500 m to the west (Fig. 4). The internal architecture of the trough-shaped sets is composed primarily of inclined cross-strata. Within the lowermost set, the orientation of cross-strata varies systematically across the trough from 338° at its south-eastern limit to 080° at its north-western limit. Superimposed within this trough is a smaller (110-m-wide) trough-shaped bounding surface onto which overlying cross-strata downlap. Several other smaller scale troughs (50–110 m wide) occur either superimposed on or within large-scale sets. The orientation of cross-strata within both the smaller and larger troughs is variable, although





the mean direction for both is towards the north-east. The lowermost set at locality 1c is at least 30 m thick, whereas overlying sets are 5–12 m thick.

**Interpretation.** The surface that defines the base of the Main Aeolian Unit is a supersurface representing a period of deflation and the formation of erosional relief (Mountney *et al.*, 1999a). Deflation on this surface is the result of aeolian winnowing of sand- and silt-grade material to leave a concentrated lag of granules and pebbles. These pebbles were originally transported into the region via ephemeral stream flow (Mountney *et al.*, 1999a). The sand-filled polygonal fracture networks represent the desiccation and cracking of a formerly damp surface and may signify aeolian deflation down to the level of the water table, as a result of a similar mechanism to that described for the Jurassic Page Sandstone of Arizona (Kocurek *et al.*, 1991). There is, however, no evidence of bacterial or fungal binding of the sediment surface, nor are there any signs of early pedogenesis or evaporite precipitation.

The horizontally laminated deposits that overlie the supersurface are wind-ripple laminae (translatent strata in the terminology of Hunter, 1977). Overlying inclined cross-strata are alternating grainflow and grainfall laminae that represent the slipface deposits of aeolian bedforms. The 52-m-thick basal set represents a minimum value for the height of these bedforms (Rubin & Hunter, 1982). Cross-strata that extend continuously from the top of the set to close to its base signify simple draa-scale bedforms with active slipfaces (Brookfield, 1977). The low-angle,

upwind-dipping, laterally extensive bounding surfaces are interdune migration surfaces (Kocurek, 1996), while the overlying, low-angle, wind-ripple deposits are flat interdune areas between the aeolian bedforms. While the interdune migration surfaces are exposed as gently inclined, upwind-dipping, planar features in sections orientated parallel to the palaeowind direction (locality 1a), their three-dimensional architecture is only revealed in sections orientated perpendicular to the palaeowind direction (localities 1b and 1c). Here, they take the form of large-scale troughs that indicate significant crestline sinuosity to the major aeolian bedforms (Fig. 5). The wavelength of this sinuosity is at least the width of the troughs (up to 500 m). The degree of curvature of the sinuosity is at least the variation in the orientation of the cross-strata within a single trough ( $102^\circ$  for the large trough at locality 1c). The geometry, scale and fill of these features is similar to the 'superscoops' described from the Jurassic Navajo Sandstone of Utah by Blakey (1988a). The low points in each trough represent the result of scouring into the previously deposited aeolian accumulation by migrating scour pits. The vertical arrangement of these trough-shaped features is well exposed at locality 1b where the offset nature of the stacking indicates that successive bedforms migrated across the region with crestline sinuosities that were  $\approx 180^\circ$  out-of-phase (for a theoretical example, see Rubin, 1987; fig. 34a).

The inclined, downwind-dipping bounding surfaces exposed between the interdune migration surfaces at locality 1a are superimposition surfaces (Kocurek, 1996), indicating the migration

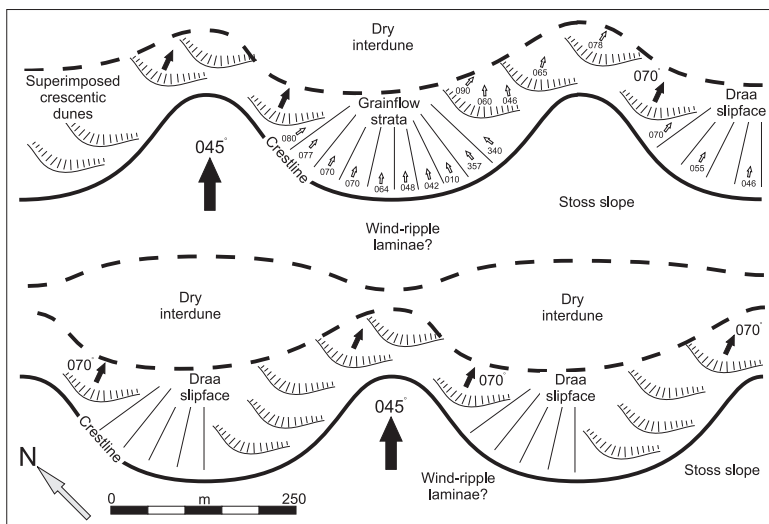


**Fig. 5.** Plan-view reconstruction of the morphology of the original dune and draa bedforms at locality 1 based on bounding surface and cross-strata orientations recorded in Fig. 4.



of superimposed secondary bedforms down the lee slope of larger scale primary bedforms. The mean orientation of the cross-strata (towards  $060^\circ$ ) that is bounded by the superimposition surfaces is  $15^\circ$  clockwise relative to the  $045^\circ$  orientation of the superimposition surfaces themselves. This signifies that the secondary bedforms migrated obliquely towards  $070^\circ$  across the lee slope of the primary bedforms, rather than directly down their lee slope (Rubin & Hunter, 1983, 1985; Clemmensen & Blakey, 1989; Fig. 5). At localities 1b and 1c, the superimposition surfaces take the form of small troughs that, like their larger counterparts, again signify the presence of along-crestline sinuosity, but this time of the secondary bedforms. The wavelength of the crestline sinuosity of these secondary bedforms is 50–110 m, whereas the amount of slipface curvature is up to  $40^\circ$ . The superimposed forms are therefore interpreted to be oblique crescentic dunes (Fig. 5).

The geometric information presented in Fig. 4 has been used to reconstruct the main morphological elements of the original bedforms at locality 1 (Fig. 6). This has been achieved using the quantitative geometric model of Rubin (1987). The bedforms are similar in morphology to the crescentic draas described from the Jurassic Entrada Sandstone of Utah by Kocurek (1981a,b).

### Sedimentary architecture in the mid-basin region (locality 2)

*Description.* Locality 2 lies 14 km to the south-east of locality 1, is 600 m wide, 130 m high and orientated NE–SW, parallel to the palaeowind direction (Fig. 7). The base of the Main Aeolian Unit is marked by a laterally continuous, near-horizontal bounding surface characterized by quartz granules and pebbles. The lowermost set in the overlying succession is 8–35 m thick (increasing in a downwind direction) and is characterized by 1–2 m of low-angle, planar laminated deposits that pass vertically into cross-strata inclined up to  $25^\circ$  towards the north-east. At the base of this set, three small channel features, each 2–4 m wide and 1–2 m deep, are exposed (Fig. 7). These features have steep margins that cut into adjacent low-angle, planar laminated deposits. Their internal fill is largely homogeneous sandstone, with a texture similar to that of adjacent laminated deposits. One of the channels is partially filled with a 1-m-wide block of sandstone with angular margins

and an internal architecture similar to that of adjacent deposits. A laterally extensive bounding surface defines the top of the 8- to 35-m-thick set. This surface climbs in a downwind direction at  $2.6^\circ$  relative to the basal bounding surface (Fig. 7). Apart from the three small channels, the internal architecture of the basal set is relatively simple, being characterized predominantly by simple cross-strata. In at least three places, however, downwind-dipping bounding surfaces truncate these cross-strata. Overlying cross-strata do not downlap onto these bounding surfaces but are instead aligned parallel to them. Several 8- to 15-m-thick sets of cross-strata overlie the basal set and are defined by bounding surfaces that climb at low angles in a downwind direction. The basal 1 m of each set is locally, but not everywhere, characterized by low-angle laminated sandstones that steepen upwards to merge with steeply inclined cross-strata.

*Interpretation.* The extensive bounding surface at the base of the Main Aeolian Unit is again interpreted to be a deflationary supersurface because of the concentration of gravel and pebbles upon it (Mountney *et al.*, 1999a). The overlying low-angle, planar laminated deposits are wind-ripple strata indicative of deposition in a dry interdune environment. These laminae pass vertically into grainflow and grainfall cross-strata that signify deposition via avalanching and suspension settling on the lee face of an advancing aeolian bedform. The presence of three minor channels at this point of transition from interdune to dune slipface represents the product of an ephemeral and spatially isolated fluvial flash-flood event. Rapid fluvial run-off associated with a desert storm would be sufficient to erode the 1- to 2-m-deep channels into the loosely consolidated interdune deposits. The channels are most probably located at the boundary between the interdune and dune slope deposits because the topography of the aeolian dune acted as a barrier to overland flow and directed the run-off along the flanks of the dune. This behaviour is common in the Sossusvlei region of the modern Namib Desert (Lancaster & Teller, 1988) and has been documented from the Sinai Peninsula (Sneh, 1983). Alternatively, the presence of the channels could be related to a pause in aeolian sedimentation. The channels are filled with locally derived well-sorted and rounded aeolian sand. The homogeneous nature of the channel fill represents the rapid deposition of both bedload

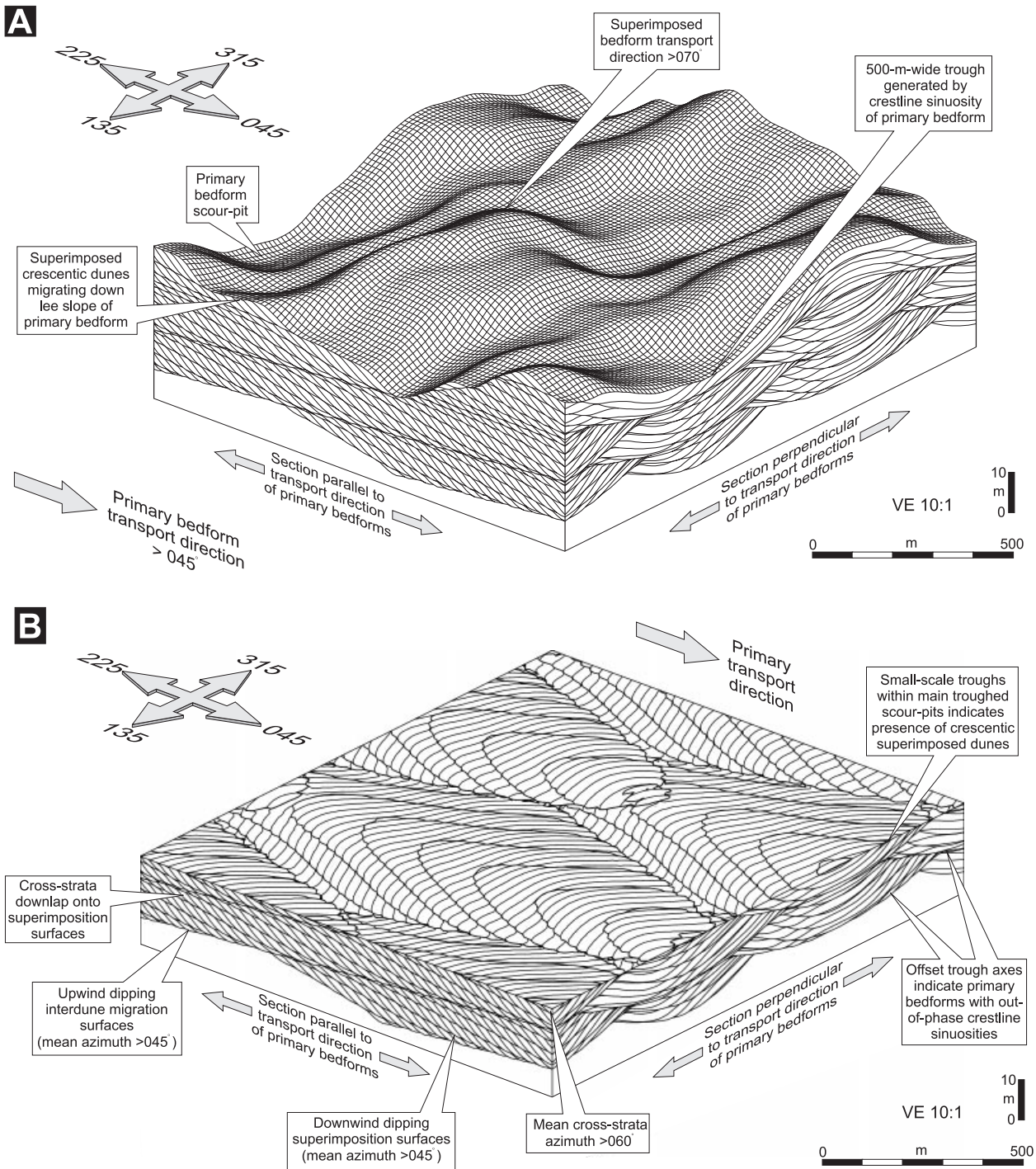


**Fig. 6.** Computer-generated model of the compound draa with oblique superimposed crescentic dunes responsible for generating the sets preserved at locality 1. Model results obtained using the program of Rubin (1987). Primary bedforms migrate towards 045°, have crestline sinuosities with a wavelength of 500 m and an amplitude of 75 m. The large, off-set stacked troughs are generated by the climb of successive primary bedforms with crestline sinuosities that are 180° out-of-phase. Superimposed secondary bedforms migrate 25° clockwise relative to the primary bedforms (i.e. towards 070°). These secondary bedforms have crestline sinuosities with a wavelength of 200 m and an amplitude of 20 m. All input parameters are taken from Fig. 4. (A) Surface section view. (B) Horizontal section view.

and suspended sediment load as a result of rapid waning of the storm flow and infiltration into the highly permeable interdune sands. The inclined

angular sandstone block in one of the channels represents a bank-collapse feature and signifies some degree of competence within the interdune

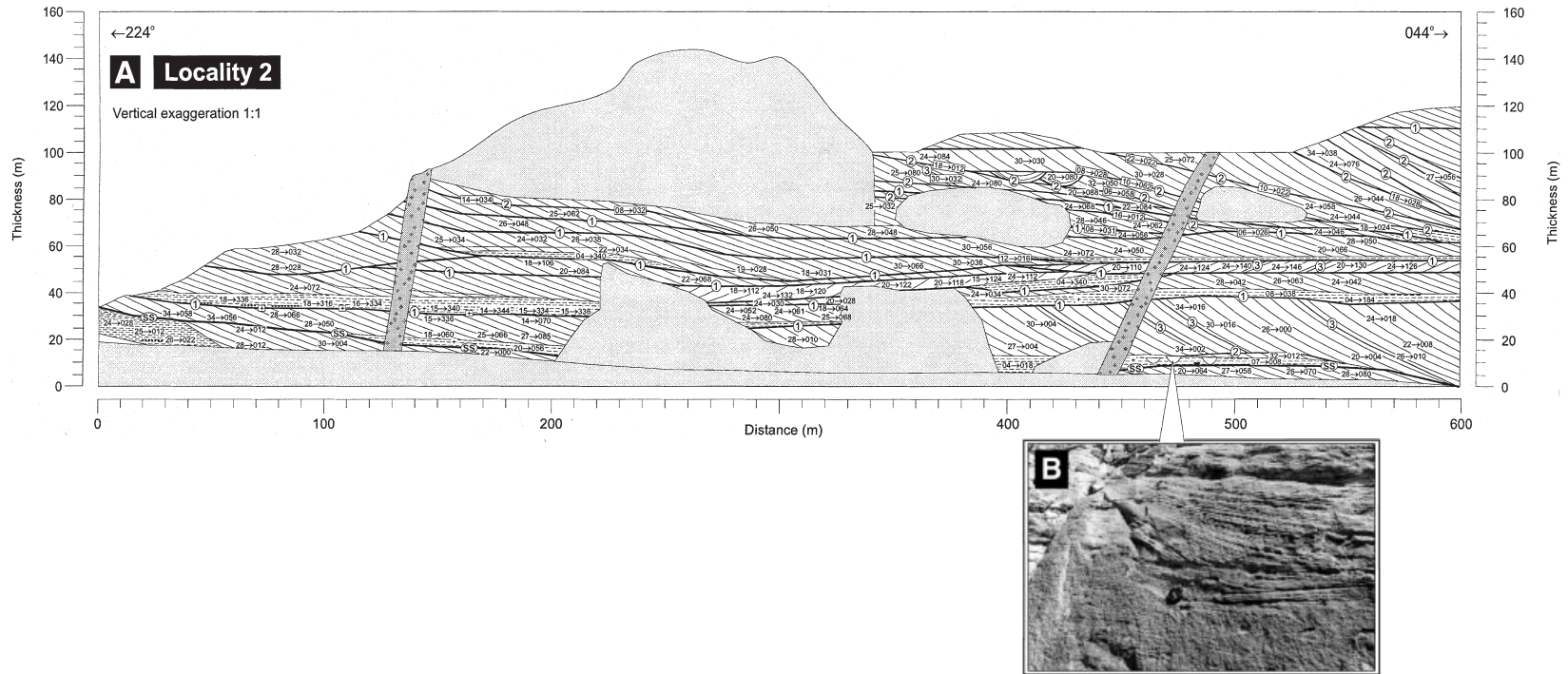


**Fig. 7.** (A) Architectural element analysis panel depicting set geometry and bounding surface relationships at locality 2 (mid-basin region). Note the inclination of the interdune migration surfaces relative to the supersurface at the base of the succession. Strata portrayed in this panel are exclusively aeolian in origin except for three small fluvial channels (highlighted). See Fig. 4 for key. (B) Detail of the margin of one of the fluvial channels. Note the erosive contact with the adjacent horizontally laminated wind-ripple strata. The inclined strata that comprises the channel fill is a bank-collapse feature. Lens cap diameter = 5 cm.

substrate comprising the channel banks. Such competence in soft sediments may be achieved by wetting of the sand, possibly by the rainfall event itself.

### Sedimentary architecture in the Huab Outliers region (locality 3)

*Description.* The three-dimensional architecture of the Main Aeolian Unit further towards the southerly basin margin is well exposed around the base of a series of mountains termed the Huab Outliers (Fig. 1). A distinctive surface with a granule and pebble lag, polygonal fractures and locally abundant burrows (Fig. 8) defines the base of the unit. Burrows are 15–100 cm long, vertical to subvertical, unlined, filled with fine to medium sand and display no internal structure. The outcrop is 1200 m long and trends NE–SW (parallel to the palaeowind direction), exposing a relatively simple bounding surface architecture (Fig. 9). Two complete aeolian sets and the base of a third are exposed within the cliff section. Set 1 directly overlies the basal surface and attains a maximum thickness of 10 m at the north-eastern end of the section, thinning to 0 m some 450 m to the SW. The upper margin of this set is defined by a laterally extensive bounding surface that rises off the basal bounding surface and climbs towards the NE (downwind). The internal set architecture is composed predominantly of simple cross-strata, although several minor bounding surfaces are present. The basal 1 m of set 1 is composed of low-angle, planar laminated sandstone. Set 2 overlies set 1 and is consistently 8 m thick, characterized by steeply inclined cross-strata, with an upper boundary defined by a laterally extensive bounding surface that climbs in a downwind direction. Tracing this bounding surface down-dip (SW), it intersects with the basal bounding surface at the base of the Main Aeolian Unit.

*Interpretation.* The basal bounding surface is again interpreted to be a supersurface. The overlying sets represent the deposits of migrating aeolian bedforms. The widespread presence of grainflow and grainfall cross-strata within these sets is indicative of deposition on the active lee face of the bedforms. Grainflow strata together with a lack of superimposition bounding surfaces within these sets indicates that the lee slope of the original bedforms was at the angle-of-repose.

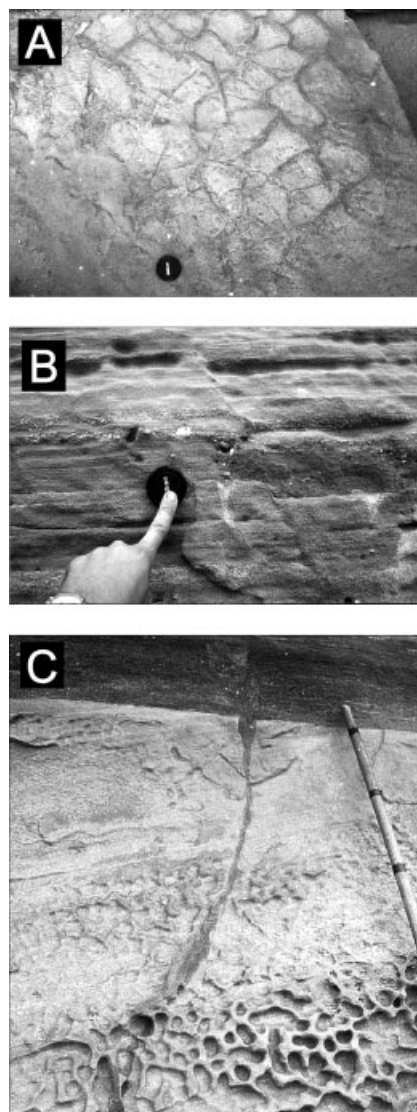


**Fig. 8.** Characteristic features of the supersurface at the base of the Main Aeolian Unit at locality 3. (A) Polygonal fractures in plan view. Lens cap for scale. (B) Burrows in cross-section view. (C) Burrows in cross-section view. Note the distinctive change in sediment character across the surface. Lens cap diameter = 5 cm. Divisions on measuring pole = 20 cm.

### Sedimentary architecture in the Huab Outliers region (locality 4)

*Description.* The basal bounding surface at locality 4 can be traced 4 km back to locality 3, confirming its lateral extent. The surface is again characterized by a granule and pebble lag, fractures and burrows. The bounding surface architecture of the overlying succession is more complicated than that observed at locality 3 and is composed of a series of stacked sets bounded by erosive surfaces that truncate underlying sets



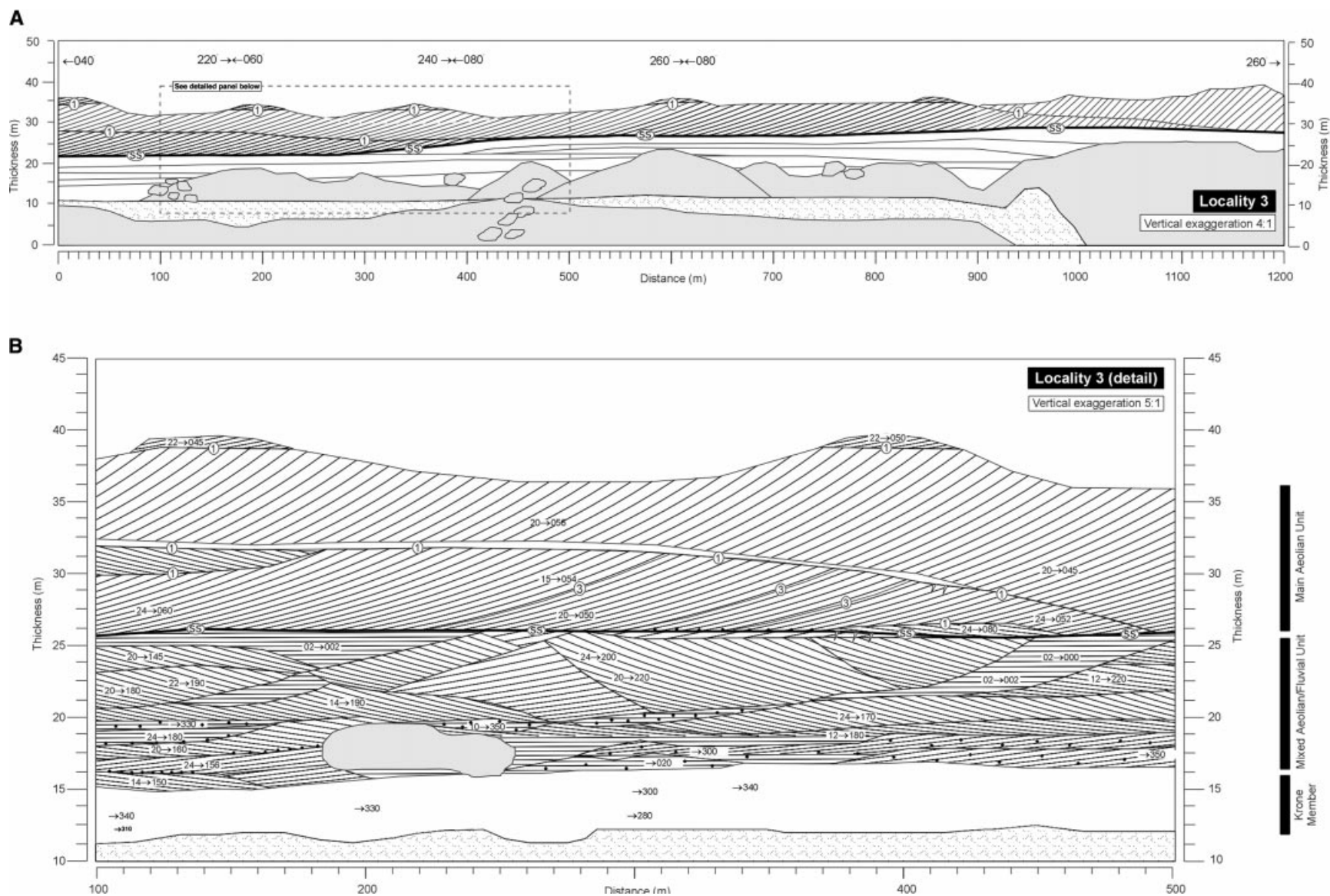


**Fig. 9.** (A) Architectural element analysis panel depicting set geometry and bounding surface relationships at locality 3 (Huab Outliers region). Note the inclination and lateral spacing of the interdune migration surfaces relative to the supersurface at the base of the Main Aeolian Unit. (B) Detail of the eastern part of locality 3. Note the change in architecture between the Mixed and Main Aeolian Units. See Fig. 4 for key.

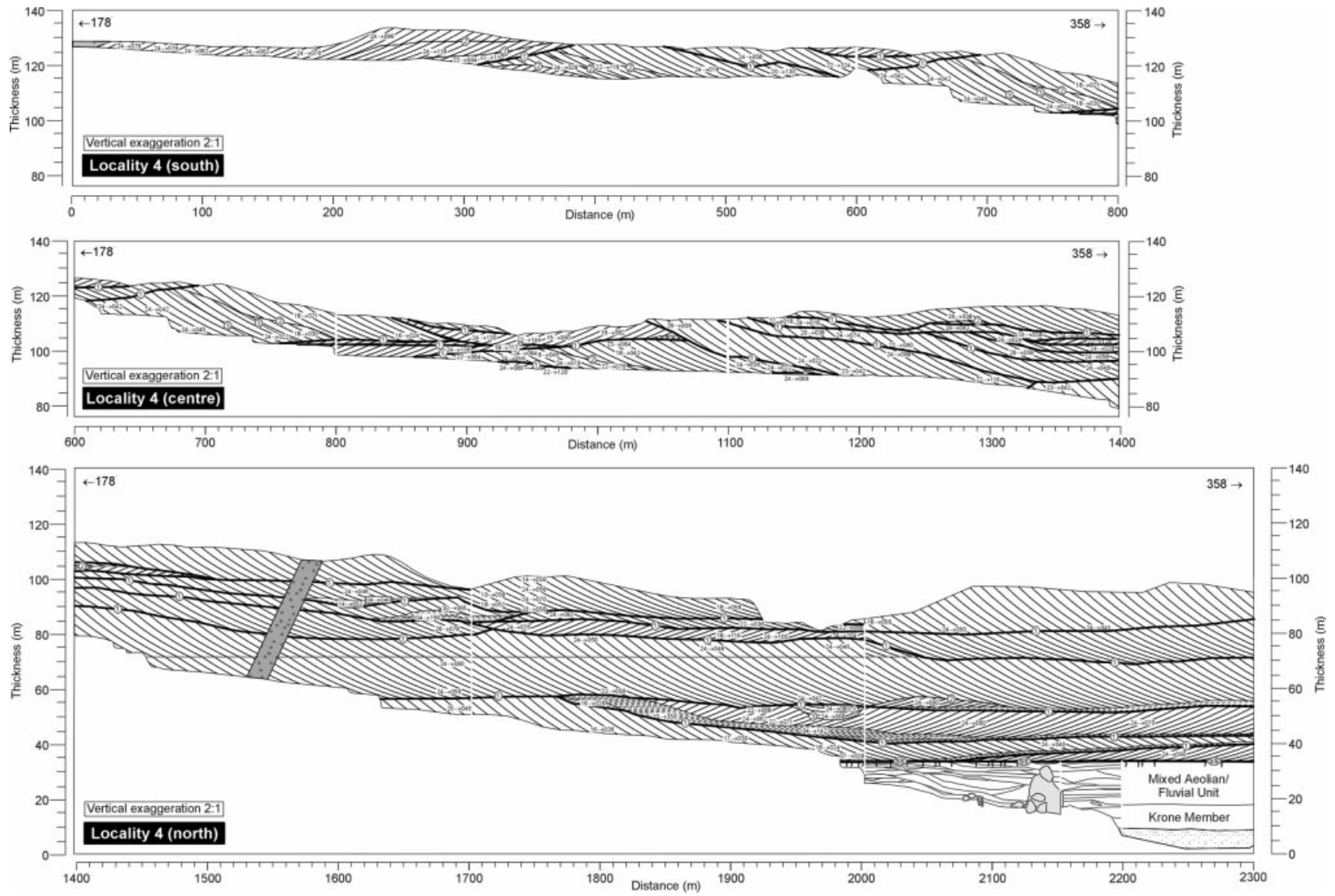


Fig. 10. Architectural element analysis panel depicting set geometry and bounding surface relationships at locality 4 (Huab Outliers region). See Fig. 4 for key.



in the succession (Fig. 10). Sets thicken and pinch to form lens-shaped bodies in outcrop. Individual sets vary in thickness, up to a maximum of 22 m, although higher up the succession individual sets do not exceed 10 m. The internal architecture of sets throughout the succession is sometimes complicated by the presence of downwind-dipping bounding surfaces onto which overlying cross-strata downlap.

*Interpretation.* The lateral continuity of the basal surface confirms its interpretation as a regionally extensive superset. The complexity in the overlying bounding surface architecture reflects the N–S orientation of the section, which is oblique to palaeo-transport direction. The pinching and thickening of individual sets and the truncational nature of the bounding surfaces indicate the presence of original aeolian bedforms with some degree of crestline sinuosity (Rubin & Hunter, 1983). The presence of downwind-dipping bounding surfaces is indicative of the superimposition of secondary bedforms on the lee slopes of the primary bedforms (compound cross-bedding) and suggests that the primary bedforms in this region did not always maintain an active slipface (Brookfield, 1977).

#### **Sedimentary architecture at the southern basin margin (locality 5)**

*Description.* The Main Aeolian Unit at the southern basin margin is restricted in thickness to 50 m. At locality 5, the base of the unit is characterized by a pebble lag and displays a relief of 18 m over a distance of 800 m (Fig. 11). Overlying deposits consist of six laterally continuous simple sets of aeolian strata. The basal 50–100 cm of most sets is composed of horizontally laminated deposits that grade up into inclined cross-strata. The thickness of each set is relatively uniform (8–10 m).

*Interpretation.* Each of the six sets represents the deposits of a simple, transverse aeolian bedform, and the bounding surfaces that separate the sets represent interdune migration surfaces. The horizontal deposits that overlie the bounding surfaces are wind-ripple strata, indicative of a low-angle plinth that advanced in front of the migrating bedforms. The inclined cross-strata are composed predominantly of grainflow laminae that signify the development of slipfaces on the lee slope of the advancing dunes.

#### **STRATIGRAPHY OF THE UPPER AEOLIAN UNIT**

Deposits of the Upper Aeolian Unit are distinct from those comprising the underlying Main Aeolian Unit because they accumulated during or after the initial eruption of basaltic lava in the region (Mountney *et al.*, 1998; Jerram *et al.*, 1999). Deposits of the Upper Aeolian Unit vary in thickness from zero to 100 m in the Huab Basin and may lie directly on deposits of the Main Aeolian Unit or may be separated from them by the initial Etendeka flood basalts. The sedimentary and bounding surface architecture of the Upper Aeolian Unit is described and interpreted with reference to two type localities that occupy central and marginal positions within the basin respectively (Figs 1 and 2).

#### **Sedimentary architecture in the basin depocentre (locality 6)**

*Description.* Locality 6 is located in the basin depocentre, 6 km from locality 1, and comprises a 600-m-wide outcrop that reveals the internal architecture of a 90-m-high, aeolian bedform preserved largely intact after rapid inundation by flood basalts (Fig. 12). This bedform lies directly on, and is conformable with, the uppermost deposits of the Main Aeolian Unit. It is characterized by a stoss slope that dips at 15°, against which the overlying basalt lava flow onlaps, and a lee slope that dips at 24° towards 030° (trends 120°). Basalt-filled low points bound both the upwind and the downwind limits of the bedform, which is 600 m in downwind extent. The internal architecture of the bedform is characterized by a series of downwind-dipping bounding surfaces that are distinct from and truncate well-developed cross-stratification planes. The cross-strata themselves display a mean dip direction towards 055°. The downwind-dipping surfaces all downlap onto a higher order bounding surface that defines the base of the bedform. The bedform overlies a series of three near-horizontal aeolian cross-stratified sets that vary in thickness from 6 m to 15 m.

*Interpretation.* The low points that bound both the upwind and the downwind limits of the bedform are interdune hollows. The downwind-dipping bounding surfaces that comprise the internal architecture of the bedform are superimposition surfaces and indicate the presence of a

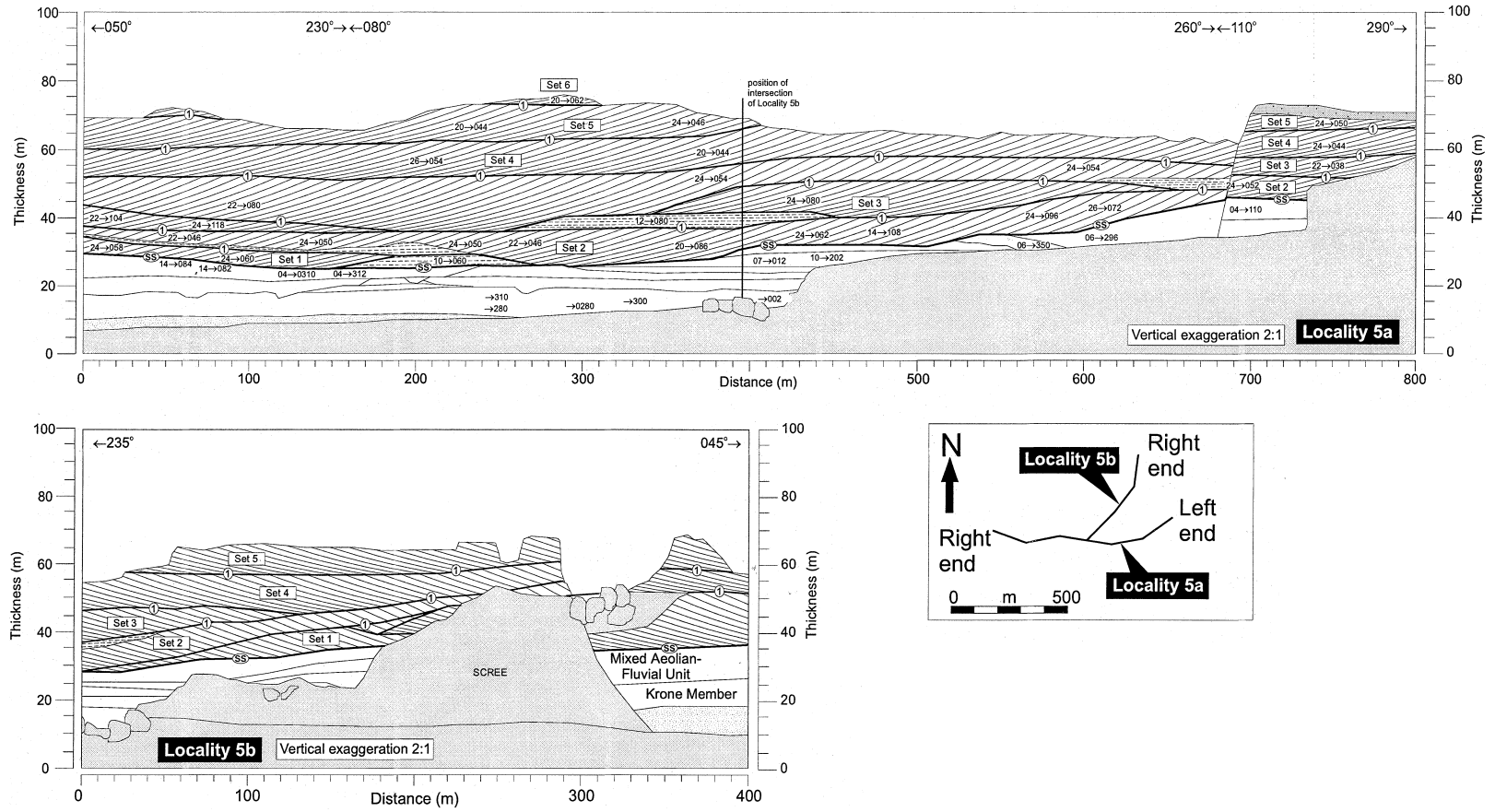
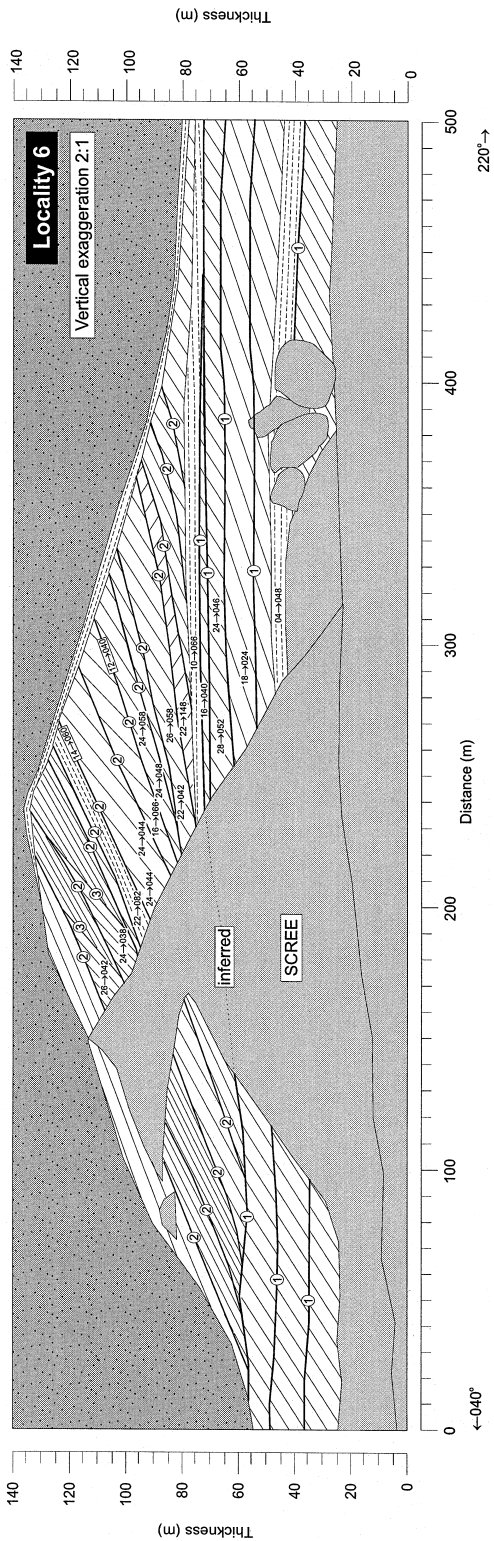


Fig. 11. Architectural element analysis panel depicting set geometry and bounding surface relationships at locality 5 (southern basin margin). See Fig. 4 for key.



**Fig. 12.** Architectural element analysis panel depicting set geometry and bounding surface relationships at locality 6 (basin depocentre). This locality exposes a 90-m-high, 600-m-wavelength compound transverse draa preserved intact after burial by Etendeka flood basalts. Note the presence of superimposition surfaces that steepen in a downwind direction. These record a transition from slipfaceless to slipfaced draa through time. See Fig. 4 for key.

draa, over which smaller dunes migrated (McKee, 1979). The narrow range of dip orientations of cross-strata within the bedform signifies the migration to the north-east of superimposed bedforms over the surface of a larger parent bedform (Mountney *et al.*, 1999b). The mean orientation of cross-strata (055°) is 25° clockwise of the 030° migration direction of the main bedform, signifying a component of oblique transport of the superimposed bedforms (Rubin & Hunter, 1983). The superimposed dunes are of transverse type and migrated down the lee slope of the parent bedform to generate a compound draa morphology according to the terminology of McKee (1979).

**Sedimentary architecture at the southern basin margin (locality 7)**

*Description.* Locality 7 is located close to the southerly basin margin, 4 km from locality 5, and comprises a 700-m-wide outcrop that reveals the internal architecture of a 56-m-high aeolian bedform preserved partly intact (Ward, 1989). This bedform lies directly on, and is conformable with, the uppermost deposits of the Main Aeolian Unit. The internal architecture comprises cross-strata that extend throughout the thickness of the bedform and dip at up to 26° towards N-E. Individual cross-stratification planes can be traced up to 250 m along strike. Several minor bounding surfaces are present, with inclinations and orientations only slightly different from the cross-strata that they truncate.

*Interpretation.* The narrow range of dip orientations of cross-strata within this bedform signifies the migration to the north-east of a transverse draa. The presence of cross-strata that extend throughout the thickness of the bedform indicates the presence of a well-developed slipface subject to grainflow avalanching. The minor bounding surfaces are reactivation surfaces associated with realignment of the slipface, probably associated with minor changes in the prevailing wind direction.

**RELATING PRESERVED SET THICKNESS TO ORIGINAL BEDFORM SIZE**

Individual cross-stratified sets described from the Main Aeolian Unit of the Etjo Formation vary considerably in thickness from just a few metres to

a maximum of 52 m (Fig. 4). To what extent is the preserved thickness of these aeolian sets determined by the size of the original bedforms? The assumption that larger bedforms will generate thicker sets is not necessarily valid. For deposits of migrating aeolian bedforms to become incorporated into the rock record, the bedforms must climb at a positive angle with respect to a generalized sediment surface (Rubin & Hunter, 1982). It is the angle-of-climb, together with the original bedform size (expressed as downwind wavelength), that determines preserved set thickness.

### Bedform climbing

If bedforms migrate through an aeolian system, and the mass or volume of sediment entering the system at the upwind margin is greater than that leaving at the downwind margin, then the system has a positive net sediment budget (Kocurek & Havholm, 1993). For dry aeolian systems that are not influenced by the water table and where the depositional surface has 100% sand dune cover, a positive net sediment budget will result in the onset of bedform climbing, whereby bedforms and their bounding surfaces move upwards (positive climb) with respect to a generalized sediment surface (Fig. 13A), which is defined as a smooth surface passing midway between the troughs and crests of the bedforms (Rubin & Hunter, 1982). A positive angle-of-climb is the

mechanism by which most aeolian dune deposits become incorporated into the rock record. For dry aeolian systems with less than 100% sand dune cover, a positive net sediment budget will cause existing dunes to grow as they migrate, filling the interdune spaces (Fig. 13B), but will not usually result in a positive angle-of-climb until the interdune hollows have been filled by the growing dunes (Wilson, 1971). Aeolian bedforms in wet aeolian systems, in which the water table or its capillary fringe are in contact with the depositional surface (Kocurek & Havholm, 1993), may experience a positive angle-of-climb even when sand dune cover is less than 100%, but only where there is a rise in water table (either absolute because of a change in climate, or relative as a result of subsidence), allowing new preservation space to be generated (Loope & Simpson, 1991; Crabaugh & Kocurek, 1993; Carr-Crabaugh & Kocurek, 1998; Fig. 13C).

For bedforms of a given size and morphology, the angle-of-climb is the key parameter that determines the thickness of sets that accumulate after the passage of the bedforms; steeper angles-of-climb result in thicker preserved sets. Studies of modern deserts (Wilson, 1973; McKee, 1979) indicate that large aeolian bedforms (dunes and draas) nearly always undergo low rates of vertical accumulation in comparison with downwind migration rates and hence exhibit very low (subcritical) angles-of-climb at angles consider-

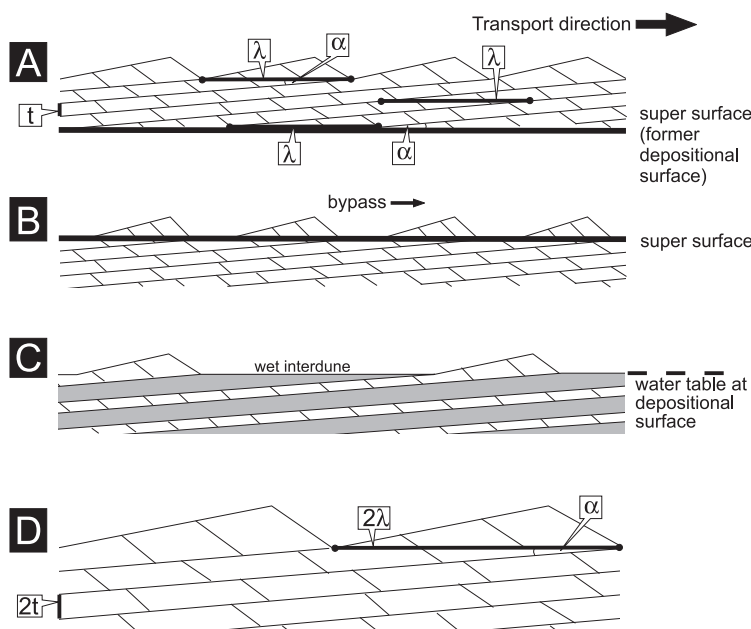


**Fig. 13.** Models for bedform climbing. (A) Dry aeolian system with 100% loose sand cover (positive angle-of-climb).  $\lambda$  = downwind bedform wavelength,  $\alpha$  = angle-of-climb,  $t$  = preserved set thickness. Note that wavelength can be measured between successive interdune hollows, along a former depositional surface or between successive interdune migration surfaces in an alignment parallel to the former depositional surface. (B) Dry aeolian system with <100% loose sand cover (bedforms grow filling interdunes, but angle-of-climb is zero). (C) Wet aeolian system with water table rise (angle-of-climb controlled by rate of rise of water table vs. rate of bedform migration). (D) Angle-of-climb is the same as in (A) but bedform wavelength =  $2\lambda$ . Resulting preserved set thickness =  $2t$ .

ably less than the inclination of the stoss slope of the bedform (Hunter, 1977). Subcritical climbing results in only partial preservation of the basal portion of the original bedform, and the preserved set is therefore only a record of the processes that operated in the basal region of the original bedform.

### Distinguishing between the effects of bedform climb and bedform size

Along with the angle of bedform climb, bedform size (expressed as downwind wavelength) is the other parameter that controls the thickness of climbing strata that are left behind after the migration of a bedform across an area. For a given angle-of-climb, larger bedforms will generate thicker sets (Fig. 13D). Determining the significance of the angle of bedform climb vs. the size of the original bedforms in controlling preserved set thickness is a fundamental problem in aeolian sedimentology because direct measurement of either of these values is often not possible. As stated above, the angle of bedform climb can only be measured with respect to a former depositional surface (Rubin & Hunter, 1982). Similarly, determining downwind bedform wavelength within sets of aeolian strata also requires the establishment of a former depositional surface. Identifying such a surface in the preserved rock record requires special circumstances.

Some of the problems of determining angle-of-climb and former bedform wavelength are illustrated by studies of the Jurassic Entrada Sandstone of Utah. Kocurek (1981b) and Crabough & Kocurek (1993) demonstrated that aeolian sets within the Entrada Sandstone, with an average vertical thickness of 4 m, climb at an angle of  $0.3^\circ$  in a downwind direction, relative to the uppermost tidal deposits of the underlying Carmel Formation. These tidal deposits were important because they were interpreted to represent a former depositional surface. The downwind distance between successive interdune bounding surfaces that climb off the tidal deposits is a direct measure of original bedform wavelength (850 m for the lowermost deposits in the Entrada). Higher up the succession, the average thickness of the preserved sets increases to 6 m. This must mean that either the angle of bedform climb has increased or the size of the bedforms has increased. However, establishing which is the case is not possible because there is no local 'former depositional surface' to use as a reference datum in this part of the succession.

### Bedform climb and bedform size in the Etjo Formation

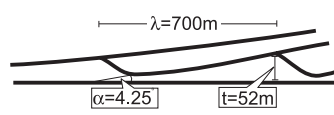
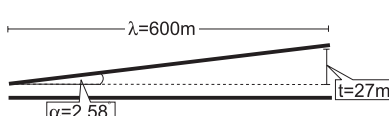
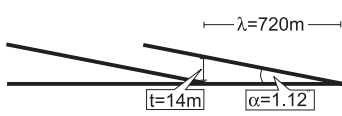
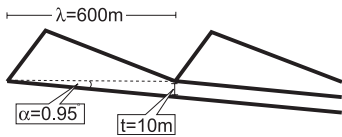
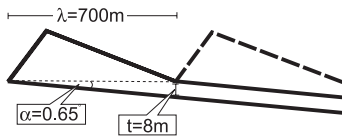
*The base of the Main Aeolian Unit.* Of interest in the Etjo Formation is the systematic spatial variation in the thickness of the bottommost set in the Main Aeolian Unit. In the basin depocentre (locality 1), the basal set is 52 m thick. In the mid-basin region (locality 2), the basal set is 35 m thick. Further towards the basin margin, in the Huab Outliers region (localities 3 and 4), the basal set reaches 10–22 m in thickness. At the basin margin itself (locality 5) the basal set is only 8–10 m thick. This trend is confirmed elsewhere in the basin by the 70 high-resolution logs. The question then arises as to whether this variation in preserved set thickness at the base of the Main Aeolian Unit primarily reflects changes in the angle of bedform climb around the basin, or changes in original bedform size around the basin. This question can be answered by identifying a former depositional surface within the basal part of the succession. The supersurface at the base of the Main Aeolian Unit represents an erosional feature generated by a period of deflation during a break in the accumulation of the Etjo Formation (Mountney *et al.*, 1999a). The resumption of aeolian activity in the basin is represented by the accumulation of the bottommost sets in the overlying Main Aeolian Unit. These sets represent the deposits of aeolian bedforms that climbed off the supersurface, which itself represents a former depositional surface. Although the supersurface has local relief of up to 20 m, over distances of 1–2 km the feature is essentially planar and can be used as a reference datum from which to measure both the angle-of-climb and the wavelength of the original bedforms.

The downwind distance between the points at which successive interdune migration surfaces climb off a supersurface is a direct measure of original bedform wavelength (Fig. 13A). At the base of the Etjo Formation, localities 1a, 2 and 3 all exhibit interdune migration surfaces that climb off the basal supersurface. Estimates of original bedform wavelengths for these localities vary from 600 to 1000 m (owing to difficulty in determining the exact point at which the migration surfaces climb off the supersurface). For each of these localities, the most likely original bedform wavelength is 700–750 m and, importantly, bedforms that accumulated in the basin depocentre (locality 1) were not significantly larger than those that accumulated in the mid-basin and

Huab Outlier regions (localities 2 and 3). This indicates that it was the angle of bedform climb at the time of deposition that controlled the thickness of the sets that were preserved. At localities 2 and 3, the angles-of-climb can be measured directly and are  $2.6^\circ$  and  $1.1^\circ$  respectively. At locality 1, the angle-of-climb has been determined to be somewhat steeper ( $3.0\text{--}4.3^\circ$ ) using the simple trigonometric relationship between bedform wavelength and preserved set thickness (Fig. 14). These measurements indicate that a decrease in the angle of bedform climb from the basin depocentre towards the southerly basin margin (rather than a decrease in the size of the bedforms themselves) is responsible for the observed decrease in preserved set thickness.

*The top of the Main Aeolian Unit.* With the exception of localities at the basin margin, basal sets within the Main Aeolian Unit range from 14 to 52 m in thickness. In contrast, overlying sets in

the succession attain only 5–15 m in thickness. For a given locality, does this upward decrease in preserved set thickness therefore primarily reflect temporal changes in the angle of bedform climb or temporal changes in original bedform size? Once again, this question can be answered by identifying a former depositional surface, but this time within the upper part of the succession. The style of termination of aeolian accumulation within the Huab Basin (drowning of the erg by the rapid emplacement of extensive flood basalts) is unique (Jerram *et al.*, 1999). The flood basalts have preserved large-scale aeolian bedforms intact at the top of the Etjo Formation and, in so doing, have made it possible to relate sets of climbing cross-strata directly to the actual bedforms responsible for their generation (Mountney *et al.*, 1999b). The draa preserved beneath the lava at locality 6 occupies a basin depocentre position and has a wavelength of 600 m and a height of 90 m (Figs 12 and 14). The downwind wavelength of this bedform is therefore similar to

Locality	Observed relationship	Downwind wavelength (m)	Preserved set thickness (m)	Angle of climb (deg)	Comments
1a		700	52	4.25 *	Estimates of downwind wavelength vary from 700–1000 m. Basal supersurface used to define former depositional surface.
		1000	52	2.98 *	
2		600	27	2.58	Estimates of downwind wavelength vary from 600–1000 m. Basal supersurface used to define former depositional surface.
		1000	45 *	2.58	
3		720	14	1.12	Direct measurement of downwind wavelength. Basal supersurface used to define former depositional surface.
6		600	10	0.95	All parameters well constrained. Successive interdune hollows used to define former depositional surface.
5/7		700	10	0.82 *	Downwind wavelength poorly constrained. Successive interdune hollows used to define former depositional surface.
		700	8	0.65 *	
		1000	8	0.46 *	

**Fig. 14.** Calculated angles-of-climb ( $\alpha$ ), downwind bedform wavelengths ( $\lambda$ ) and preserved set thicknesses ( $t$ ) for the main study localities in the Huab Basin. Where bedform wavelength is poorly constrained, most likely and maximum feasible estimates are made. \*Signifies parameter value determined trigonometrically. Bedform size is largely independent of position within the basin, whereas angle-of-climb is greatest at the base of the succession in the basin depocentre and decreases both spatially towards the basin margin and temporally up-succession.



the bedforms at the base of the Main Aeolian Unit. Both the upwind and the downwind limits of this draa terminate in lava-filled depressions interpreted to be interdune hollows. The deposits of this bedform can be traced upwind to a point at which they form a 10-m-thick set (Mountney *et al.*, 1999b) that was preserved by positive, but subcritical, bedform climbing immediately before lava inundation. The two interdune hollows define a former depositional surface (Fig. 13A), from which an angle-of-climb of  $1.0^\circ$  has been determined (Fig. 14), a value considerably less than the  $3.0\text{--}4.3^\circ$  determined for the base of the Main Aeolian Unit in the basin depocentre.

At the southern basin margin, the large aeolian bedform exposed at locality 7 is also interpreted to have been inundated by flood basalts. This bedform has a wavelength of at least 700 m and a height of at least 56 m, making it of similar size to the bedform at locality 6 in the basin depocentre. Importantly, preserved sets at the southern basin margin are typically only 8–10 m thick (Fig. 11), indicating that the angle-of-climb of this large bedform cannot have exceeded  $0.7\text{--}0.8^\circ$  at the time of lava inundation (Fig. 14). Evidence from localities 6 and 7 indicates that, as for the base of the Etjo Formation, low angles of bedform climb (rather than small bedforms) are responsible for the preservation of only thin sets in the upper parts of the Etjo Formation.

## DISCUSSION: ACCOMMODATION SPACE IN AEOLIAN SYSTEMS

Both spatial and temporal changes in the angle of bedform climb within the Etjo erg were responsible for variations in the architecture preserved in the rock record. This raises the question of what controls the angle of bedform climb at the basin or erg scale? Positively climbing aeolian systems require a positive net sediment budget (Rubin & Hunter, 1982; Kocurek & Havholm, 1993). At the erg scale, Kocurek & Lancaster (1999) identified three separate factors that define the sediment state (sediment budget) of an aeolian system: (1) an upwind supply of sediment needs to be generated; (2) some or all of this sediment needs to be available for downwind transport, and (3) the transport capacity of the wind itself will dictate how much of this sediment can be moved. For a positive net sediment budget to exist within an erg system, the amount of sediment available for transport needs to decrease downwind, or the

transport capacity of the wind needs to decrease downwind; one or both conditions will promote accumulation.

In the Etjo Formation, the upwind supply of sediment was provided by the extensive Botucatu erg, deposits of which cover much of present-day Brazil. The Etjo system formed a downwind extension of this large sand-sea (Bigarella, 1970; Dingle *et al.*, 1983) and, consequently, there was an ample upwind supply of sediment for constructing the Etjo erg. Furthermore, the sediment supplied by the Botucatu erg took the form of well-sorted, well-rounded, spherical, predominantly dry, loose aeolian sand grains that would have been readily entrained and transported by the wind. Grain transport is unlikely to have been impeded by the binding of grains to a damp surface or the presence of extensive vegetation in the arid environment of the Botucatu sand-sea. Thus, sediment availability (the susceptibility of surface grains to entrainment by the wind) was unlikely to have been a limiting factor in the evolution of the Etjo erg. This leaves the transport capacity (sediment-carrying capacity) of the wind as a control on erg accumulation.

Before the onset of deposition of the Main Aeolian Unit, the basin was largely sediment starved. Winds blowing across the basin were deflationary and responsible for generating the superelevation at the base of the Main Aeolian Unit. The combination of ongoing aeolian deflation, coupled with movement on extensional faults in the tectonically active basin, would have generated a topographic depression that remained unfilled (Fig. 15A). As the upwind Botucatu erg grew, prevailing south-westerly winds would have moved sand into the Huab Basin. Winds entering the basin are likely to have been fully saturated in terms of sediment load. The actual sediment transport rate would have equalled the maximum potential transport rate (Kocurek & Havholm, 1993) at the upwind margin of the basin. Winds moving into the area of unfilled basin topography would undergo downwind deceleration resulting from expansion of the airflow (Wilson, 1973; Fryberger *et al.*, 1979; Mainguet & Chemin, 1983), resulting in a decrease in the transport rate and promotion of bedform growth (George & Berry, 1993). Aeolian bedforms within the basin would expand to fill interdune hollows and, with continued sediment supply, would begin to climb over one another, preserving sets (Fig. 15B). The angle-of-climb would be greatest in the basin depocentre where maximum wind deceleration resulting from flow

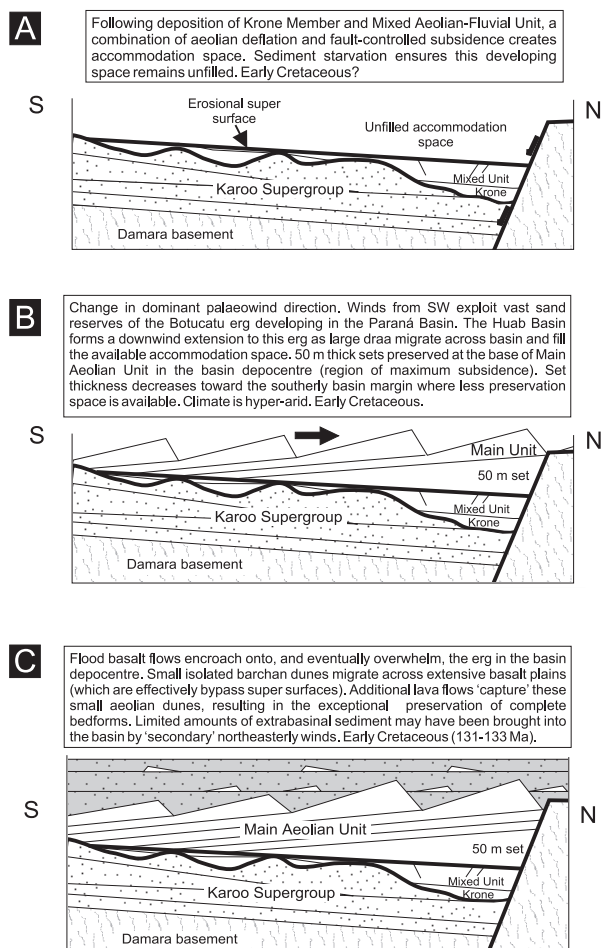


**Fig. 15.** Model for the evolution of the Etjo erg. (A) An unfilled topographic depression in the developing basin forms as a result of sediment starvation, deflation of pre-existing deposits and ongoing subsidence. (B) Initial influx of aeolian sand, sourced from the Botucatu erg of the Paraná Basin that lay upwind. Rapid infilling of the available accommodation space. High angles of bedform climb result in the preservation of thick sets in the basin depocentre. (C) Continued high rates of sediment supply, but the limited availability of accommodation space inhibits bedform climbing, resulting in the preservation of thinner sets despite the presence of large aeolian draa within the basin. Erg activity terminated by eruption of Etendeka Flood basalts. Figure not to scale.

expansion would occur. Preservation space in the topographic hollow of the basin depocentre would also be at a maximum. The accumulation of thick sets in the basin depocentre would fill the topographic hollow, promoting acceleration of the airflow moving across the basin (Blakey, 1988b). Flow acceleration decreases the net sediment budget back towards neutral, reflected by bedforms that climb at lower angles and preserve

thinner sets (Fig. 15C). If the accumulation built sufficiently, it would attain an equilibrium height (Wilson, 1971), whereby the removal of sediment at the downwind margin would equal supply at the upwind margin: the angle-of-climb would reduce to zero, the sediment budget would be neutral and a bypass supersurface would be generated (Kocurek & Havholm, 1993). However, in the case of the Etjo Formation, lava inundation blanketed the erg, terminating the aeolian system.

## CONCLUSIONS

Aeolian sets preserved in the Main Aeolian Unit were deposited by transverse draa up to 90 m high and with downwind wavelengths of 600–1000 m (Fig. 16). These bedforms were either simple or compound in form (McKee, 1979). The simple draa are represented by 5- to 52-m-thick sets of large-scale planar or trough cross-bedded strata with asymptotic toesets. These units are encountered across the basin. The compound draa are represented by 20- to 50-m-thick sets and are confined to the basin depocentre and mid-basin regions. The presence of superimposition surfaces indicates that the primary bedforms commonly lacked an active slipface and were instead characterized by a low-angle lee slope down which superimposed crescentic dunes migrated. The orientation of the superimposition surfaces, relative to cross-strata bounded by them, indicates that the superimposed forms migrated up to 25° clockwise (obliquely) over the parent bedforms. The set architecture at locality 1 records the evolution of the bedform from a slipfaced form (simple grain-flow cross-strata) to a slipfaceless form with superimposed dunes migrating down its lee slope. Conversely, the set architecture at locality 6 records the evolution of a slipfaceless form (with superimposed dunes) to a slipfaced form (Mountney *et al.*, 1999b). Crestline sinuosities varied in wavelength from at least 50–110 m for the superimposed dunes to at least 500 m for the larger draa. Small, flat-lying interdune regions occupied elliptical hollows directly in front of the advancing draa (Fig. 16). The size of the draa did not vary substantially across the Huab Basin region and was most probably controlled by the long-term, regional sand budget. In contrast, the smaller scale dunes superimposed on these draa varied in morphology depending on local (possibly seasonal) changes in sand budget (Lancaster, 1988).

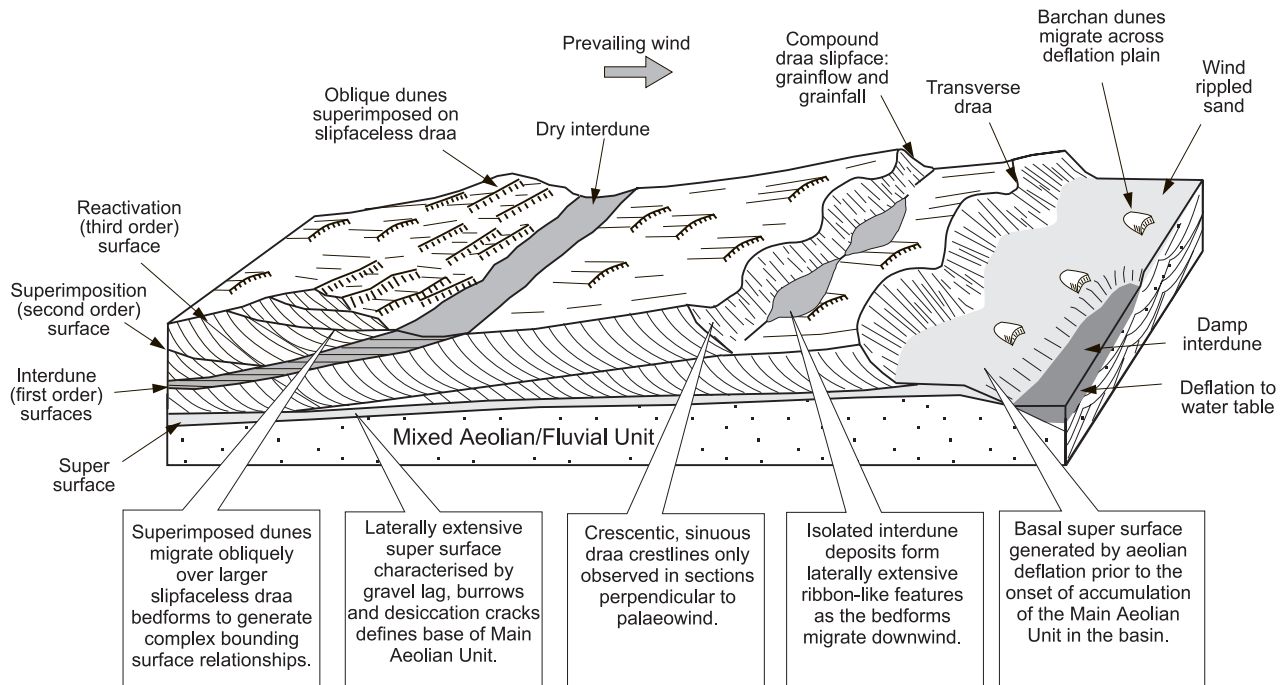


Fig. 16. Cartoon reconstruction of a portion of the active Etjo erg in the Huab Basin depocentre.

Original downwind bedform wavelengths were relatively constant across the basin, indicating that the substantial variations in preserved set thickness are directly attributable to variations in the angle of bedform climb. Importantly, the presence of a former depositional surface (a supersurface) at the base of the succession and completely preserved draa-scale bedforms at the top of the succession enable preserved set thickness to be related to both the angle of bedform climb and the original bedform size. This is significant because it confirms that both spatial and temporal variations in preserved set thickness in the Etjo Formation are primarily the result of changes in angle of bedform climb and that draa-scale aeolian bedforms occurred throughout the Huab Basin region and throughout the evolution of the main Etjo erg. The preservation of a 52-m-thick set at the base of the succession in the basin depocentre reflects the availability of accommodation space at the time of onset of aeolian erg building. Spatial and temporal changes in the availability of accommodation space are considered to be the fundamental mechanisms responsible for controlling preserved aeolian architecture in high-sediment supply, dry aeolian systems such as the Etjo Formation.

## ACKNOWLEDGEMENTS

We are grateful to BG plc and Conoco UK Ltd for sponsoring this research. Gary Kocurek, Mike Talbot and Jim Best are thanked for their encouraging reviews. We thank Dougal Jerram (Durham University), Steve Flint, Ian Stanistreet (University of Liverpool), Simon Milner (Geological Survey of Namibia) and Harald Stollhofen (University of Würzburg) for their helpful discussions, and the Geological Survey of Namibia for the use of its facilities.

## REFERENCES

- Allen, J.R.L. (1968) *Current ripples*. North Holland, Amsterdam, 433 pp.
- Anderson, R.S. (1988) The pattern of grainfall deposition in the lee of aeolian dunes. *Sedimentology*, **35**, 175–188.
- Bigarella, J.J. (1970) Continental drift and palaeocurrent analysis (a comparison between Africa and South America). In: *Proceedings Paper IUGS 2nd Gondwana Symposium*, pp. 73–97. Pretoria, South Africa.
- Blakey, R.C. (1988a) Superscoops: Their significance as elements of eolian architecture. *Geology*, **16**, 483–487.
- Blakey, R.C. (1988b) Basin tectonics and erg response. *Sedim. Geol.*, **56**, 127–151.
- Brookfield, M.E. (1977) The origin of bounding surfaces in ancient aeolian sandstones. *Sedimentology*, **24**, 303–332.

- Carr-Crabaugh, M.** and **Kocurek, G.** (1998) Continental sequence stratigraphy of a wet eolian system: a key to relative sea-level change. In: *Relative Role of Eustasy, Climate and Tectonism in Continental Rocks* (Eds K. Shanley and P. McCabe), *SEPM Spec. Publ.*, **59**, 213–228.
- Clemmensen, L.B.** and **Blakey, R.C.** (1989) Erg deposits in the Lower Jurassic Wingate Sandstone, northeastern Arizona: oblique dune sedimentation. *Sedimentology*, **36**, 449–470.
- Crabaugh, M.** and **Kocurek, G.** (1993) Entrada Sandstone: an example of a wet aeolian system. In: *The Dynamics and Environmental Context of Aeolian Sedimentary Systems* (Ed. K. Pye), *Geol. Soc. London, Spec. Publ.*, **72**, 103–126.
- Dingle, R.V.** (1992) Structural and sedimentary development of the continental margin off Southwestern Africa. *Commun. Geol. Surv. Namibia*, **8**, 35–43.
- Dingle, R.V., Siesser, W.G.** and **Newton, A.R.** (1983) *Mesozoic and Tertiary Geology of Southern Africa*. Balkema, Rotterdam, 375 pp.
- Frets, D.C.** (1969) Geology and structure of the Huab-Welwitschia area, South West Africa. *Bull. Precamb. Res.*, **5**, 235 pp.
- Fryberger, S.G.** and **Schenk, C.J.** (1988) Pin stripe lamination – A distinctive feature of modern and ancient eolian sediments. *Sedim. Geol.*, **55**, 1–15.
- Fryberger, S.G., Ahlbrandt, T.S.** and **Andrews, S.** (1979) Origin, sedimentary features, and significance of low-angle eolian ‘sand sheet’ deposits, Great Sand Dunes National Monument and vicinity, Colorado. *J. Sedim. Petrol.*, **49**, 733–746.
- George, G.T.** and **Berry, J.K.** (1993) A new lithostratigraphy and depositional model for the Upper Rotliegend of the UK sector of the Southern North Sea. In: *Characterization of Fluvial and Aeolian Reservoirs* (Eds C.P. North and D.J. Prosser), *Geol. Soc. London, Spec. Publ.*, **73**, 291–319.
- Hodgson, F.D.I.** (1970) The geology of the Karoo system in the Southern Kaokoveld, South West Africa. In: *Proceedings Paper IUGS 2nd Gondwana Symposium*, pp. 233–240. Pretoria, South Africa.
- Hodgson, F.D.I.** (1972) *The Geology of the Brandberg – Aba Huab Area, South West Africa*. Unpublished PhD Thesis, University of Orange Free State, South Africa.
- Horsthemke, E.** (1992) Fazies der Karoosedimente in der Huab-Region, Damaraland, NW-Namibia. *Gottinger Arb. Geol. Palaont.*, **55**, 102 pp.
- Horsthemke, E., Ledendecker, S.** and **Paroda, H.** (1990) Depositional environments and stratigraphic correlations of the Karoo sequence in Northwestern Damaraland. *Commun. Geol. Surv. Namibia*, **6**, 63–75.
- Hunter, R.E.** (1977) Basic types of stratification in small eolian dunes. *Sedimentology*, **24**, 361–387.
- Hunter, R.E.** (1981) Stratification styles in eolian sandstones: some Pennsylvanian to Jurassic examples from the Western Interior USA. In: *Recent and Ancient Non-Marine Depositional Environments: Models for Exploration* (Eds F.G. Ethridge and R.M. Flores), *SEPM Spec. Publ.*, **31**, 315–329.
- Jerram, D.A., Mountney, N.P.** and **Stollhofen, H.** (1999) Facies architecture of the Etjo Sandstone Formation and its interaction with the basal Etendeka flood basalts of NW Namibia: Implications for offshore analogues. In: *Oil and Gas Habitats of the South Atlantic* (Eds N. Cameron, R. Bate and V. Clure), *Geol. Soc. London, Spec. Publ.*, **153**, 367–380.
- Kocurek, G.** (1981a) Erg reconstruction: The Entrada Sandstone (Jurassic) of northern Utah and Colorado. *Palaeogeogr., Palaeoclimatol., Palaeoecol.*, **36**, 125–153.
- Kocurek, G.** (1981b) Significance of interdune deposits and bounding surfaces in aeolian dune sands. *Sedimentology*, **28**, 753–780.
- Kocurek, G.** (1988) First-order and super bounding surfaces in eolian sequences – bounding surfaces revisited. *Sedim. Geol.*, **56**, 193–206.
- Kocurek, G.** (1996) Desert aeolian systems. In: *Sedimentary Environments: Processes, Facies and Stratigraphy* (Ed. H.G. Reading), 125–153. Blackwell Science, Oxford.
- Kocurek, G.** and **Havholm, K.G.** (1993) Eolian sequence stratigraphy – a conceptual framework. In: *Siliciclastic Sequence Stratigraphy* (Eds P. Weimer and H.W. Possa-mentier), *AAPG Mem.*, **58**, 393–409.
- Kocurek, G.** and **Lancaster, N.** (1999) Aeolian system sediment state: Theory and Mojave Desert Kelso dune field example. *Sedimentology*, **46**, 477–504.
- Kocurek, G., Knight, J.** and **Havholm, K.** (1991) Outcrop and semi-regional three-dimensional architecture and reconstruction of a portion of the eolian Page Sandstone (Jurassic). In: *The Three-Dimensional Facies Architecture of Terrigenous Clastic Sediments and its Implications for Hydrocarbon Discovery and Recovery* (Eds A.D. Miall and N. Tyler), *SEPM Concepts in Sedimentol. Paleontol.*, **3**, 25–43.
- Lancaster, N.** (1988) Controls on eolian dune size and spacing. *Geology*, **16**, 972–975.
- Lancaster, N.** and **Teller, J.T.** (1988) Interdune deposits of the Namib Sand Sea. *Sedim. Geol.*, **55**, 91–107.
- Ledendecker, S.** (1992) Stratigraphie der Karoosedimente der Huabregion (NW Namibia) und deren korrelation mit zeit-äquivalenten sedimenten des Paranabeckens (Sudamerika) und der Großen Karoo Beckens (Sudafrika) unter besonderer berücksichtigung der überregionalen geodynamischen und klimatischen entwicklung Westgondwanas. *Gottinger Arb. Geol. Palaont.*, **54**, 87 pp.
- Light, M.P.R., Maslanyj, M.P., Greenwood, R.J.** and **Banks, N.L.** (1993) Seismic sequence stratigraphy and tectonics offshore Namibia. In: *Tectonics and Seismic Sequence Stratigraphy* (Eds G.D. Williams and A. Dobb), *Geol. Soc. London, Spec. Publ.*, **71**, 163–191.
- Loope, D.B.** and **Simpson, E.L.** (1991) Significance of thin sets of eolian cross-strata. *J. Sedim. Petrol.*, **62**, 849–859.
- McKee, E.D.** (1979) *A Study of Global Sand Seas*. Geological Survey Professional Paper 1052. US Government Printing Office, Washington.
- Maignet, M.** and **Chemin, M.-C.** (1983) Sand seas of the Sahara and Sahel: an explanation of their thickness and sand dune type by the sand budget principle. In: *Eolian Sediments and Processes* (Eds M.E. Brookfield and T.S. Ahlbrandt), *Dev. Sedimentol.*, **38**, 353–363.
- Milner, S.C., Duncan, A.R., Whittingham, A.M.** and **Ewart, A.** (1995) Trans-Atlantic correlation of eruptive sequences and individual silicic volcanic units within the Paraná-Etendeka igneous province. *J. Volcanol. Geoth. Res.*, **69**, 137–157.
- Mountney, N.P., Howell, J.A., Flint, S.S.** and **Jerram, D.A.** (1998) Aeolian and alluvial deposition within the Mesozoic Etjo Sandstone Formation, NW Namibia. *J. Afr. Earth Sci.*, **27**, 175–192.
- Mountney, N.P., Howell, J.A., Flint, S.S.** and **Jerram, D.A.** (1999a) Climate, sediment supply and tectonics as controls on the deposition and preservation of the aeolian-fluvial Etjo Sandstone Formation, Namibia. *J. Geol. Soc., London*, **156**, 771–779.
- Mountney, N.P., Howell, J.A., Flint, S.S.** and **Jerram, D.A.** (1999b) Relating eolian bounding-surface geometries to the

- bed forms that generated them: Etjo Formation, Cretaceous, Namibia. *Geology*, **27**, 159–162.
- Porter, M.L.** (1986) Sedimentary record of erg migration. *Geology*, **14**, 497–500.
- Renne, P.R., Glen, J.M., Milner, S.C. and Duncan, A.R.** (1996) Age of Etendeka flood volcanism and associated intrusions in Southwestern Africa, *Geology*, **24**, 659–662.
- Rubin, D.M.** (1987) Cross-bedding, bedforms and paleocurrents. *SEPM Concepts Sedimentol. Paleontol.*, **1**, 187 pp.
- Rubin, D.M. and Hunter, R.E.** (1983) Reconstructing bedform assemblages from compound crossbedding. In: *Eolian Sediments and Processes* (Eds M.E. Brookfield and T.S. Ahlbrandt), *Dev. Sedimentol.*, **38**, 407–427.
- Sneh, A.** (1983) Desert streams in the Sinai Peninsula. *J. Sedim. Petrol.*, **53**, 1271–1279.
- Talbot, M.R.** (1985) Major bounding surfaces in aeolian sandstones – a climatic model. *Sedimentology*, **32**, 257–265.
- Ward, J.D.** (1989) *Aeolianites of the Mesozoic Etjo Formation, Damaraland and Contemporary Dunes of the Skeleton Coast*. Field Guide ‘Dunes 89’, Excursion 4b. Geological Survey, Windhoek, Namibia.
- Wilson, I.G.** (1971) Desert sandflow basins and a model for the development of ergs. *Geogr. J.*, **137**, 180–199.
- Wilson, I.G.** (1973) Ergs. *Sedim. Geol.*, **10**, 77–106.
- Zalan, P.V., Wolff, S., Astolfi, M.A.M., Vieira, I.S., Conceição, J.C.J., Appi, V.T., Neto, E.V.S., Cerqueira, J.R. and Marques, A.** (1991) The Paraná Basin, Brazil. In: *Interior Cratonic Basins* (Eds M.W. Leighton, D.R. Kolata, D.F.A. Oltz and J.J. Eidel). *AAPG Mem.*, **51**, 681–708.

*Manuscript received 30 July 1999;  
revision accepted 15 November 1999.*